International Journal of Biological Macromolecules 340 (2026) 150106

Contents lists available at ScienceDirect

International Journal of Biological Macromolecules

journal homepage: www.elsevier.com/locate/ijbiomac

Insight into novel biochemical features and function of novel antifungal GH16-β-glucanase from *Bacillus velezensis*

D. Vela-Corcia [a,b,*], A. de Vicente [b], A. Pérez-García [a,b], D. Romero [a,b,*]

[a] Instituto de Hortofruticultura Subtropical y Mediterránea "La Mayora", Universidad de Málaga – Consejo Superior de Investigaciones Científicas (IHSM-UMA-CSIC), Spain

[b] Departamento de Microbiología, Universidad de Málaga, Bulevar Louis Pasteur 31 (Campus Universitario de Teatinos), Málaga, 29071, Spain

ARTICLE INFO

Keywords:
β-Glucanase
β-Glucan
Fungal cell wall degradation
Bacillus velezensis
Botrytis cinerea
Biocontrol
Plant-microbe interaction

ABSTRACT

β-Glucanases play a critical role in degrading fungal cell wall β-glucans, compromising fungal integrity and development. Here we characterize BvlzGluc, a novel β-glucanase from *Bacillus velezensis* CECT 8237 with potent and specific activity against β-1,3-glucans. The enzyme hydrolyzes yeast-derived β-glucan but is inactive against β-1,6- and β-1,3/1,4-linked polysaccharides, such as laminarin and lichenin, indicating strict substrate specificity. Mass spectrometry of *Botrytis cinerea* cell wall extracts revealed that BvlzGluc cleaves high-molecular-weight β-glucans into smaller oligosaccharides, supporting its classification as an *endo*-β-1,3-glucanase. Kinetic analysis yielded a Km of 48 μM and a Vmax of 0.026 μmol/min. Structural modeling showed a GH16 jelly roll fold lacking a classical catalytic groove, and site-directed mutagenesis of two predicted binding residues (Y36 and T216) confirmed their functional relevance. CD spectroscopy revealed that T216A disrupts folding, while Y36A retains structure but shows reduced activity. Despite its compact architecture and divergence from canonical motifs, BvlzGluc demonstrates efficient antifungal function. Its physicochemical simplicity and specificity make it a promising candidate for scalable production and targeted applications in crop protection. This work expands our understanding of bacterial glucanases and underscores the value of structurally minimal enzymes in biocontrol strategies.

1. Introduction

β-Glucans are the primary polysaccharides found in the fungal cell wall and play essential roles in providing structural integrity and rigidity [1,2]. These polysaccharides consist of β-1,3 and β-1,6 linkages that form a fibrillar network, which contributes to the overall strength and resilience of the fungal cell wall [3,4]. β-1,3-glucan forms a helical structure that acts as a scaffold, while the β-1,6 linkages connect these helices, creating a highly cross-linked matrix [4]. This combination of linkages provides both flexibility and mechanical support, allowing for the fungal cell wall to resist environmental stresses and osmotic pressure [5,6]. β-glucans are critical in fungal physiology, particularly in maintaining the integrity of the cell wall during processes such as budding, hyphal growth, and spore formation. Their synthesis and remodeling are tightly regulated by fungal cells, with β-glucanases and other enzymes involved in modulating the polymerization and depolymerization of β-glucan chains, ensuring dynamic adaptation to various environmental conditions [5].

β-Glucanases are a group of glycoside hydrolases (GHs) that catalyze the conversion of β-glycosidic bonds in β-glucans into smaller oligosaccharides, such as cello-oligosaccharides and, occasionally, glucose [7–9]. These enzymes are classified into various types based on their specific activity, including *endo*-β-1,4-glucanase (EC 3.2.1.4), endo-β-1,3(4)-glucanase (EC 3.2.1.6), and endo-β-1,3-glucanase/laminarinase (EC 3.2.1.39), among others, as categorized by the CAZy database [10]. Among these CAZy-classified enzymes, the GH16 family forms a large and functionally diverse group of glycoside hydrolases characterized by a conserved β-jelly-roll fold [11] and predominantly *endo*-acting activity on β-linked polysaccharides. The GH16 family is widely distributed across bacteria, fungi and plants. In plants, GH16 β-glucanases participate in cell wall remodeling and contribute to immune and stress responses through the hydrolysis of β-glucans, playing important roles in defense signalling and structural adaptation [12]. GH16 enzymes hydrolyse internal β-1,3- and β-1,4-glycosidic bonds in substrates such as

* Corresponding authors at: Instituto de Hortofruticultura Subtropical y Mediterránea "La Mayora", Universidad de Málaga – Consejo Superior de Investigaciones Científicas (IHSM-UMA-CSIC), Spain.

E-mail addresses: dvela@uma.es (D. Vela-Corcia), diego_romero@uma.es (D. Romero).

https://doi.org/10.1016/j.ijbiomac.2026.150106
Received 2 October 2025; Received in revised form 15 December 2025; Accepted 4 January 2026
Available online 5 January 2026

laminarin and lichenin [11,13]. Members of this family are widely distributed across bacteria, fungi, plants and algae, where they contribute to cell-wall remodeling, morphogenesis and microbial antagonism [13]. They receive great interest in industries dedicated to biofuel production, where lignocellulosic biomass must be degraded into simpler sugars (e.g., glucose and xylose) before being refined into biofuels. By breaking down these complex polymers, glucanases help unlock renewable energy from plant-derived materials, making them valuable for sustainable energy solutions [14–17]. Additionally, they have been associated with crop protection and plant defense against fungal pathogens since they hydrolyze β-glucans in fungal cell walls, thus playing a crucial role in weakening structural barriers and, ultimately, the integrity of the pathogen [18]. This degradation exposes chitin, another key component of the fungal cell wall, making it more recognizable to the plant immune system. Upon exposure, chitin triggers plant defense mechanisms, such as the production of antimicrobial compounds and the activation of systemic acquired resistance (SAR), which limits fungal spread and infection [19–21]. *Bacillus velezensis* has emerged as a significant player because of its potent antifungal activities. The presence of β-glucanases in *B. velezensis* and their ability to suppress fungal infections make these enzymes crucial components in plant protection strategies [22,23]. Diverse β-glucanases have been described in members of this bacterial species and characterized for their roles in antagonistic interactions with fungi [24,25].

In this study, we identified and characterized a novel β-glucanase, BvlzGluc, produced by *Bacillus velezensis* CECT 8237. BvlzGluc effectively degrades the β-glucan layer of fungal cell walls, compromising structural integrity and causing severe malformations that inhibit fungal development and reduce disease incidence. Our structural and functional analyses revealed that BvlzGluc has unique characteristics distinct from those of other β-glucanases in the glycoside hydrolase family, suggesting that it represents a new type of β-glucanase. These findings underscore the importance of bacterial factors in antagonistic interactions between biocontrol agents and pathogens, furthering innovative, sustainable agricultural and biotechnological pathogen control strategies that extend beyond traditional bacterial applications.

2. Materials and methods

2.1. Plant material

Melon plants (*Cucumis melo*; cultivar Rochet Panal) were grown from seeds (Semillas Fitó) at 25 °C and 60 % relative humidity under fluorescent and incandescent light at a photofluency rate of ~120 μmol $m^{-2}s^{-1}$ and a 12/12 h photoperiod.

2.2. Fungal strain—growth and inoculation of plant material

B. cinerea isolate B05.10 was cultured on potato dextrose agar (PDA, Oxoid) in a controlled-environment chamber at 20 °C under illumination with fluorescent light at a photo fluency rate of 12 μmol $m^{-2}s^{-1}$ and a 12/12 h photoperiod. Conidia were harvested from the light-grown culture in sterile distilled water containing 0.001 % (*v*/v) Triton X-100 (J.T. Baker) and filtered through a 40-μm cell strainer to remove the remaining hyphae. Cell biology studies were carried out on germinated conidia grown in potato dextrose broth (PDB, Scharlau) inoculated with a spore suspension and incubated at 28 °C for 24 h at 150 rpm.

B. cinerea plant inoculation was performed as previously described [26]. Briefly, the conidial suspension was adjusted to 10^5 conidia mL^{-1} in half-strength filtered (0.45 μm) grape juice (100 % pure organic). Melon plants that were 5–6 weeks old were used, and each leaf was inoculated with 5-μl droplets of conidial suspension ($5{\cdot}10^2$ conidia). The plants were covered with a plastic dome and placed in the growth chamber. At 72 h postinoculation, the leaves were imaged, and the lesion size was analyzed using ImageJ 2.0 software.

2.3. Stress analysis of B. cinerea B05.10: identifying active fractions and critical concentration estimation

A stress analysis of *B. cinerea* B05.10 was performed to identify the clone supernatants with antimicrobial activity. To do so, all the clones were grown in LB medium at 37 °C for 24 h at 150 rpm. Afterward, the supernatants were collected, filter sterilized and subsequently incubated with *B. cinerea* germinated spores in a 96-well microtiter plate. Then, reactive oxygen species (ROS) production was analyzed using 10 mM hydrogen peroxide as a positive control. ROS detection was performed with dihydrorhodamine 123 (DHR123, Sigma–Aldrich). The fluorescence was recorded using a plate reader (FluoStar Omega, BMG LabTech) with excitation filters at 485 nm and emission at 520 nm, and readings were taken every 10 min over a 24-h period. The experiment was stopped when the positive control became saturated.

2.4. Sequence analysis

A search was conducted in the fosmid cloned fragments for proteins that could be secreted. For this, a previously described workflow was followed [27]. Briefly, proteins with a signal peptide were searched using SignalP (https://services.healthtech.dtu.dk/service.php?SignalP-5.0), those without transmembrane domains were identified using TMHMM (https://services.healthtech.dtu.dk/service.php?TMHMM-2.0), and proteins predicted to have extracellular subcellular localization were selected using DeepLoc (https://services.healthtech.dtu.dk/service.php?DeepLoc-1.0). Finally, a comprehensive search for conserved protein domains was conducted on the selected proteins to identify functional motifs that may be critical for their activity (https://toolkit.tuebingen.mpg.de/tools/hhpred). In addition, domain annotation was performed using HMMER searches against CAZy-derived GH16 Hidden Markov Models. BvlzGluc showed highly significant matches to GH16 profiles (*E*-values <1e–40), supporting its assignment to this family.

Multiple sequence alignment was conducted via the CLC Main Workbench (Aarhus). Phylogenetic analysis was performed by MEGA software (v.11, Kumar Lab, Temple University, Philadelphia, USA) with MUSCLE as the alignment algorithm. Phylogenetic tree analysis was subsequently carried out using the maximum likelihood statistical method, which is based on the Poisson correction model. The test to assess the phylogeny used was performed by the bootstrap method with 1000 bootstrap replications.

2.5. In vitro expression and purification of B. velezensis CECT 8237 BvlzGluc

The primers 7685F44—F (5′-AAAAAGCAGGCTCTATGCGTAAAAAAATCTTAATGGCACTC-3′) and 7685F44-R.

(5′-AGAAAGCTGGGTTTATCGATTAATTTTAAAAGAGTTTGTCG-3′) were used to amplify BAMY6639_07685 (GenBank acc. no. AMQ71412) coding sequence, the amplified fragment was cloned and inserted into the entry vector pDONR207 and then transferred to the destination vector pDEST17, which incorporates a six His-tag at the N-terminus of the proteins, using the Gateway® cloning technology (Invitrogen).

For BvlzGluc expression, the plasmid pDEST17 containing the coding sequence was transformed into chemically competent *E. coli* BL21-AI cells (Invitrogen) using heat shock. Protein expression was induced with the addition of 10 mM arabinose (Sigma–Aldrich) at an OD_{600nm} of 0.4. The cells were incubated at 37 °C for 3 h and harvested by centrifugation. The cell pellet was frozen in liquid nitrogen and stored at −80 °C overnight to increase the yield of protein recovery.

For protein purification, the cell pellet was thawed, resuspended in lysis buffer (1× CellLytic™ B-Cell Lysis Reagent [Sigma–Aldrich], 1 mM protease inhibitor phenylmethylsulfonyl fluoride (PMSF) and 0.2 mg mL^{-1} Lysozyme) and incubated at room temperature for 1 h; the remaining cells were disrupted by sonication on ice using a UP100H

sonicator (Hielscher). The crude lysate was clarified by centrifugation at 8000 ×*g* for 10 min.

The resulting supernatant was passed through a 0.45-μm filter prior to protein purification via affinity chromatography using an AKTA Start FPLC system (GE Healthcare). The lysate was loaded into a HisTrap HP 5 mL column (GE Healthcare) previously equilibrated with binding buffer (50 mM Na_3PO_4 [pH 8], 0.5 M NaCl, and 10 mM imidazole). The protein was eluted with elution buffer (50 mM Na_3PO_4 [pH 8], 0.5 M NaCl, 500 mM imidazole). Next, the purified protein was loaded into a HiPrep 26/10 desalting column (GE Healthcare), and the buffer was exchanged for 20 mM Tris-HCl, pH 8, and 50 mM NaCl. Finally, the protein was concentrated by ultrafiltration using Pierce® Concentrators 20 K MWCO (Thermo Scientific) and stored at −20 °C until analysis.

Prior to further analysis, the expressed proteins were characterized by western blotting. For immunoblot analysis, purified protein was electrophoresed on 12 % SDS–PAGE gels and electrotransferred onto polyvinylidene difluoride (PVDF) membranes using the Trans-Blot Turbo electrophoretic transfer cells (Bio–Rad). The blots were probed with a 1:1000 dilution of a rabbit monoclonal anti-His-tag antibody (Rockland). The membranes were then incubated with a 1:20,000 dilution of a horseradish peroxidase-conjugated anti-rabbit antibody (Bio-Rad), and the bands were visualized by chemiluminescent detection via an enhanced chemiluminescence (ECL) western blotting analysis system (Thermo Scientific).

2.6. Germination rate and germ tube length measurement

To estimate the germination rate and measure germ tube length, *B. cinerea* spores were first prepared by collecting a spore suspension as described above, followed by adjusting the spore concentration. The spores were plated on water agar media in sterile Petri dishes in the absence or presence of BvlzGluc and spread evenly before incubation at 25 °C. Germination was monitored at regular intervals using a microscope, and a spore was considered germinated when the germ tube exceeded the spore diameter. The germination rate was determined by counting the total number of spores and the number of spores that germinated in randomly selected fields of view. Data on the germination rate and germ tube length were recorded and averaged, with experiments conducted in triplicate to ensure reproducibility.

2.7. Transmission and scanning electron microscopy

B. cinerea was fixed in 2.5 % (*v*/v) glutaraldehyde and 4 % (v/v) paraformaldehyde in 0.1 M phosphate buffer (PBS) overnight at 4 °C. The samples were postfixed in 1 % osmium tetroxide solution in PBS for 90 min at room temperature, followed by washing with PBS and 15 min of stepwise dehydration in an ethanol series (30 %, 50 %, 70 %, 90 % and 100 % twice). Between the 50 % and 70 % steps, the samples were incubated in a 2 % uranyl acetate solution in 50 % ethanol at 4 °C overnight. After dehydration, the samples were gradually embedded in low-viscosity Spurr's resin (resin:ethanol, 1:1, 4 h; resin:ethanol, 3:1, 4 h; and pure resin overnight). The sample blocks were embedded in capsule molds containing pure resin for 72 h at 70 °C. The samples were imaged under an FEI Tecnai G2 20 TWIN transmission electron microscope at an accelerating voltage of 80 kV. The images were acquired using TIA FEI Imaging Software v.4.14.

For scanning electron microscopy, after ethanol dehydration, the samples were dried with a Bal-Tec CPD 030 critical point dryer. The dried samples were coated with a thin layer of gold using a Leica EM SCD050 coater before viewing under a JEOL JSM-6490 LV microscope.

2.8. Fungal cell wall extraction and hydrolysis quantification

Germinated spores of *B. cinerea* were captured by filtration through a 40-μm filter (Corning) to collect all the biomass, which was subsequently resuspended in 1 mL of lysis buffer (10 mM Tris-HCl pH 7.4, 1 mM PMSF). A 3-mm tungsten carbide bead (Qiagen) was added. The material was then disrupted in a TissueLyser II (Qiagen) at maximum speed with a frequency of 30 cycles s^{-1} for 30 min. This step was conducted to disrupt the cell wall. After this step, the sample was centrifuged at 1000 ×*g* for 10 min at 4 °C, the supernatant was discarded, and the pellet was washed with 1 mL of solution A (1 mM PMSF). The mixture was subsequently centrifuged again at 1000 ×*g* for 10 min at 4 °C, after which the pellet was washed with 1 mL of solution B (5 % NaCl, 1 mM PMSF). This step was repeated, changing to solution C (2 % NaCl, 1 mM PMSF) and 1 mL of solution D (1 % NaCl, 1 mM PMSF). Finally, the pellet was weighed and resuspended in 100 μL of solution A. In a 96-well plate, the cell wall purification (100 μg mL^{-1}) was combined with AMQ71412.1 protein at a concentration of 20 μg mL^{-1}. The mixture was incubated at 28 °C with agitation for 24 h. Afterward, the results were analyzed via MALDI–TOF mass spectrometry.

Hydrolysis of fungal cell wall polysaccharides by BvlzGluc was quantified by measuring the release of soluble sugars using the phenol–sulfuric acid method. Cell wall material was prepared as described above.

Reactions contained 1 mg mL^{-1} fungal cell wall suspension and 0.5 μM purified BvlzGluc in 50 mM sodium phosphate buffer pH 7.0. Control reactions without enzyme contained the same amount of cell wall and buffer. Reaction mixtures were incubated at 40 °C with gentle shaking, and aliquots were withdrawn at 0, 15, 30, 60 and 120 min. Each aliquot was immediately centrifuged at 10,000*g* for 5 min at room temperature to remove insoluble material, and the supernatant was used for quantification of soluble sugars.

Briefly, supernatant aliquots were mixed 1:1 with 5 % (*w/v*) phenol in a 1.5 mL microcentrifuge tube, followed by the rapid addition of 250 μL concentrated H_2SO_4. Samples were vortexed briefly and incubated for 30 min at room temperature. Absorbance was measured at 490 nm using a microplate reader. A standard curve was prepared in parallel using glucose solutions (0–200 μg mL^{-1}) treated identically, and results were expressed as μg of glucose equivalents per mL of reaction mixture. For each condition and time point, three independent reactions were performed, and each was measured in technical duplicate.

2.9. Chitin and chitosan visualization

To evaluate the effects of BvlzGluc on the fungal cell wall, both chitin and chitosan were visualized. For chitin visualization, *Botrytis* cells that were untreated or incubated with 0.5 μM BvlzGluc for 24 h were stained with 0.05 mg mL^{-1} WGA-Alexa Fluor 488® conjugate in PBS for 1 h at room temperature. After staining, the cells were washed three times with PBS containing Tween 20 before visualization.

For chitosan visualization, Eosin Y was employed, as it binds selectively to chitosan without showing affinity for chitin [28]. Following incubation with 0.5 μM BvlzGluc, the cells were washed twice with 1 mL of McIlvaine's buffer (0.2 M Na_2HPO_4 and 0.1 M citric acid, pH 6.0), resuspended in 500 μL of the same buffer, and stained with 30 μL of Eosin Y (5 mg mL^{-1} stock; Sigma) at room temperature in the dark for 10 min, followed by two washes with 1 mL of McIlvaine's buffer to remove excess dye. Finally, the cells were resuspended in 500 μL of McIlvaine's buffer.

The samples were imaged using a Zeiss LSM880 confocal microscope equipped with a Plan-apochromatic 63×/1.4 oil immersion objective. Chitin and chitosan were visualized with excitation at 488 nm, and images were acquired for further analysis.

2.10. Carbohydrate sedimentation assay

The carbohydrate sedimentation assay was performed as previously described [29]. Briefly, 0.5 μM BvlzGluc in 20 mM Tris (pH 8.0) was mixed with 1.5 mg of chitin (NEB), chitosan (Sigma–Aldrich) or yeast β-glucan (Sigma–Aldrich) suspensions and incubated at room temperature for 2 h on an orbital shaker at 350 rpm. The same amount of protein

in Tris buffer without added carbohydrates was used as a negative control. After centrifugation (5 min, 13,000*g*), the supernatant was collected, and the pellet was washed three times with 800 μL of 20 mM Tris (pH 8.0) prior to resuspension in 2× Laemmli buffer with the addition of 5 % β-mercaptoethanol as a reducing agent (Invitrogen). The presence of BvlzGluc in different fractions was determined by western blot analysis, as described above.

2.11. Immunofluorescence microscopy

B. cinerea cells incubated with 0.5 μM BvlzGluc for 24 h were fixed with 100 % acetone for 10 min at −20 °C. After being washed with 1× PBS, the cells were blocked with blocking solution (3 % (*w/v*) BSA and 0.2 % (*v/v*) Triton X-100) for 60 min. Finally, the cells were stained for immunofluorescence using a 1:50 rabbit monoclonal anti-β-glucan primary antibody (Thermo Fisher) followed by a 1:200 GFP-conjugated goat anti-rabbit secondary antibody (Thermo Fisher). Images were obtained via visualization of the samples using a Zeiss LSM880 confocal microscope with a Plan-apochromatic 63×/1.4 oil immersion objective and acquisition with excitation at 488 nm. The cells were counterstained with the lipophilic dye FM 4–64 (Thermo Fisher) to stain the plasma membrane.

2.12. Characterization of β-glucan substrate specificity and biochemical characterization

The activity of β-glucanase (BvlzGluc) was assessed using the 3,5-dinitrosalicylic acid (DNS) method. In brief, 0.5 μM purified enzyme (quantified with Qubit) was incubated with 60 μL of 0.5 % (w/v) yeast β-glucan (Merck) at 37 °C and pH 7.0 for 30 min. After addition of 80 μL DNS reagent and boiling for 5 min, samples were cooled to room temperature, and the absorbance was measured at 540 nm. One unit (U) of β-glucanase activity was defined as the amount of enzyme required to release 1 μmol of glucose-equivalent reducing sugar per minute.

The enzymatic activity of the purified protein was evaluated against four different β-glucans in order to assess substrate specificity and potential functional differences depending on glycosidic linkage type. The substrates tested were: yeast β-glucan (predominantly β-1,3-glucan with β-1,6 branches, extracted from *Saccharomyces cerevisiae* cell walls (Merck)), which is widely used as a standard β-1,3-glucan substrate for characterising *endo*-β-1,3-glucanase activity, Scleroglucan (linear β-1,3 backbone with regular β-1,6 branches, produced by *Sclerotium rolfsii* (InvivoGen)), Pustulan (a homopolymer of β-1,6-linked glucose units, isolated from *Umbilicaria papulose* (InvivoGen)), and Laminarin (a β-1,3-glucan with β-1,6 branches, derived from *Laminaria digitata* (Merck)).

Enzyme assays were performed in 0.1 M phosphate buffer (PBS) (pH 7.5) containing 0.5 % (*w/v*) of the respective substrate and incubated with the purified enzyme at 37 °C for 30 min. The reactions were stopped by boiling for 5 min, and the release of reducing sugars was quantified using the 3,5-dinitrosalicylic acid (DNS) method with glucose as calibration standard. Enzyme activity was calculated as μmol of reducing sugars released per min per mg of protein. Substrate preference was expressed as relative activity (%) by normalizing to the activity obtained with yeast β-glucan, which was set as 100 %. All assays were performed in triplicate, and values are reported as mean ± standard deviation.

For physicochemical characterization, BvlzGluc was assayed under varying conditions. The optimal pH was determined by incubating the enzyme with 0.5 % yeast β-glucan in buffers covering pH 3.0–10.0 (citrate–phosphate, Tris–HCl, and glycine–NaOH) at 37 °C for 30 min, identifying pH 7.0 as the optimum. pH stability was tested by pre-incubating the enzyme in the same buffer systems at 25 °C for 1 h, after which residual activities were measured relative to untreated controls (100 %). The optimal temperature was determined in citrate–phosphate buffer (pH 7.0) by incubating the enzyme with substrate for 10 min at temperatures ranging from 20 °C to 90 °C.

2.13. Protein modeling and molecular docking

AlphaFold3 [30] was used for automated protein tertiary structure modeling of the *B. velezensis* CECT 8237 BvlzGluc protein. To identify potential binding sites of yeast β-glucan (β-1,3-glucan with β-1,6 branches; PubChem ID: 92024379) to the BvlzGluc protein, automated molecular docking and thermodynamic analysis were performed using the web-based SwissDock program [www.swissdock.ch/docking] [31]. SwissDock predicts the possible molecular interactions between a target protein and small molecule based on the docking algorithm EADock DSS [32]. The docking was performed using the "Accurate" parameter at otherwise default parameters, with no region of interest defined (blind docking). Binding energies were estimated by using CHARMM (Chemistry at HARvard Macromolecular Mechanics), a molecular simulation program implemented within SwissDock software, and the most favorable energies were evaluated by Fast Analytical Continuum Treatment of Solvation (FACTS). Finally, the energy results were scored and ranked by *full fitness* (kcal mol^{-1}), and spontaneous binding was exhibited by the estimated Gibbs free energy ΔG (kcal mol^{-1}). The negative values of ΔG support the assertion that the binding process is highly spontaneous. Modeling and docking results were visualized using UCSF Chimera v1.8 software.

2.14. Site-directed mutagenesis

Site-directed mutagenesis was performed using the QuikChange Lightning Multi Site-Directed Mutagenesis Kit (Agilent Technologies) according to the manufacturer's protocol. The template for mutagenesis encompassed the entire locus of the BvlzGluc gene from *B. velezensis* isolate CECT 8237 cloned into pDEST17. Residues Tyr36 and Thr216 were replaced by Ala using the primer pairs SDMY36A-F/-R and SDMT216A-F/-R, respectively, generating the pDEST17-A36 and pDEST17-A216 plasmids.

2.15. Circular dichroism spectroscopy

Circular dichroism was employed to investigate the secondary structure of the wild-type BvlzGluc enzyme and the site-directed mutants BvlzGluc-Y36A and BvlzGluc-T216A. Protein samples were prepared at a final concentration of 1 μM in 50 mM sodium phosphate buffer (pH 7.4) and equilibrated at room temperature prior to analysis. Far-UV CD spectra were recorded in the wavelength range of 190–300 nm using a quartz cuvette with a 0.3 cm path length. Measurements were performed at 25 °C with a scan speed of 200 nm min^{-1}, a bandwidth of 1 nm, and a response time of 1 s on a JASCO J-815 spectropolarimeter equipped with a Peltier temperature control system. Each spectrum was the average of three independent scans after subtraction of the buffer baseline.

Data were expressed as mean residue ellipticity ([θ], deg·cm^2·$dmol^{-1}$) and analyzed to compare the folding state of the native and mutant proteins.

2.16. Kinetic analysis of β-glucanase activity

Kinetic parameters were determined to characterize the catalytic efficiency of the enzyme using yeast β-glucan as the substrate. Assays were performed in 1× PBS buffer (pH 7.5) at 37 °C, under identical conditions to those described for the specificity tests. Yeast β-glucan was prepared at a range of concentrations from 0 to 1 mM, adjusted to ensure coverage of both subsaturating and saturating regions of the curve. The purified enzyme was diluted so that the reaction proceeded within the linear range of product formation, with less than 10 % of substrate consumed during the measurement period.

Reactions were initiated by addition of the enzyme to pre-equilibrated substrate solutions and incubated for short time intervals (5 min), with three sampling points taken for each substrate

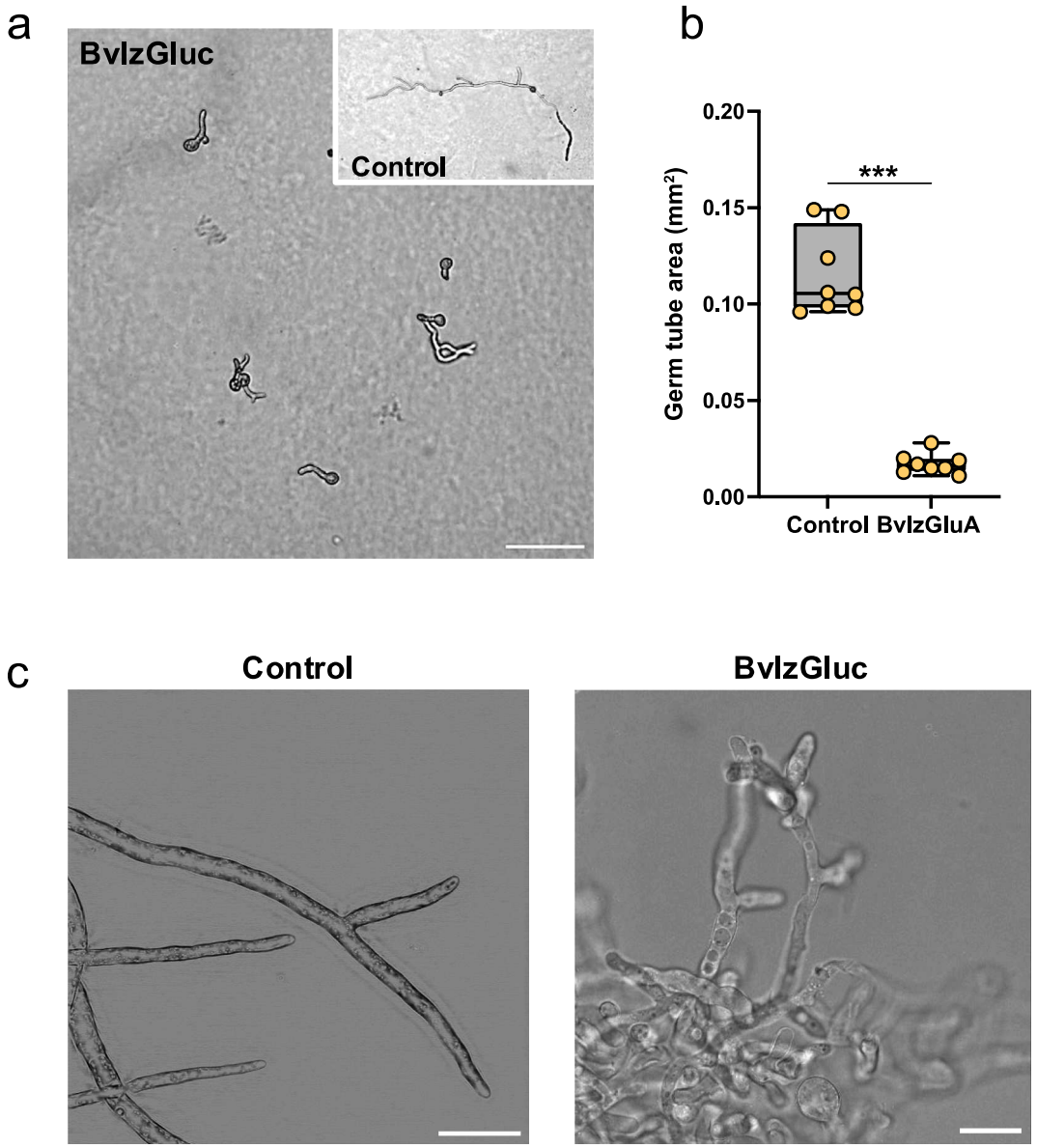

Fig. 1. Impact of BvlzGluc on *Botrytis cinerea* development. **a**. The germination of *B. cinerea* spores was significantly inhibited upon exposure to BvlzGluc. In addition to the reduction in germination rates, the length of the germ tubes also considerably decreased. Scale bar, 20 μm. **b**. Whisker plot showing the quantification of the germ tube area. All measurements (yellow dots), medians (black line), and minimum and maximum values (whisker ends) are represented. The datasets did not pass the Shapiro–Wilk test for normality ($P > 0.05$) and were compared using a nonparametric two-tailed Mann–Whitney test, with three asterisks indicating significant differences at $P < 0.001$. **c**. The effect of BvlzGluc on the development of *B. cinerea* was profound, leading to abnormal hyphal growth. The protein disrupted normal fungal development, resulting in the formation of short, highly branched hyphae. This aberrant growth pattern suggests that BvlzGluc interferes with the mechanisms that regulate hyphal elongation and branching. Scale bar, 30 μm. (For interpretation of the references to colour in this figure legend, the reader is referred to the web version of this article.)

concentration to confirm linearity. The reactions were terminated by boiling for 5 min, and the release of reducing sugars was quantified by the DNS method [33], with glucose as calibration standard. Initial velocities (v_0) were calculated from the linear increase in product formation over time and expressed as μmol of reducing sugars released per min per mg of protein.

The kinetic data (v_0 versus substrate concentration) were fitted to the Michaelis–Menten model using non-linear regression analysis (GraphPad Prism). From this analysis, apparent values of K_m and V_{max} were obtained. All assays were carried out in triplicate, and kinetic values are reported as mean ± standard deviation.

2.17. Statistical analysis

GraphPad Prism v.10.0.0 (GraphPad Software, Boston, Massachusetts, USA) was used for statistical analysis of the experimental data. When the data were normally distributed and the sample variances were equal, Student's *t*-tests were performed with Welch's correction. In all other cases, the Mann–Whitney Rank Sum test was performed. For multiple comparisons, one-way analysis of variance (ANOVA) was performed when the equal variance test was passed. In all other cases, one-way ANOVA on ranks was performed (Kruskal–Wallis significant difference test). Significance was accepted at $P < 0.05$.

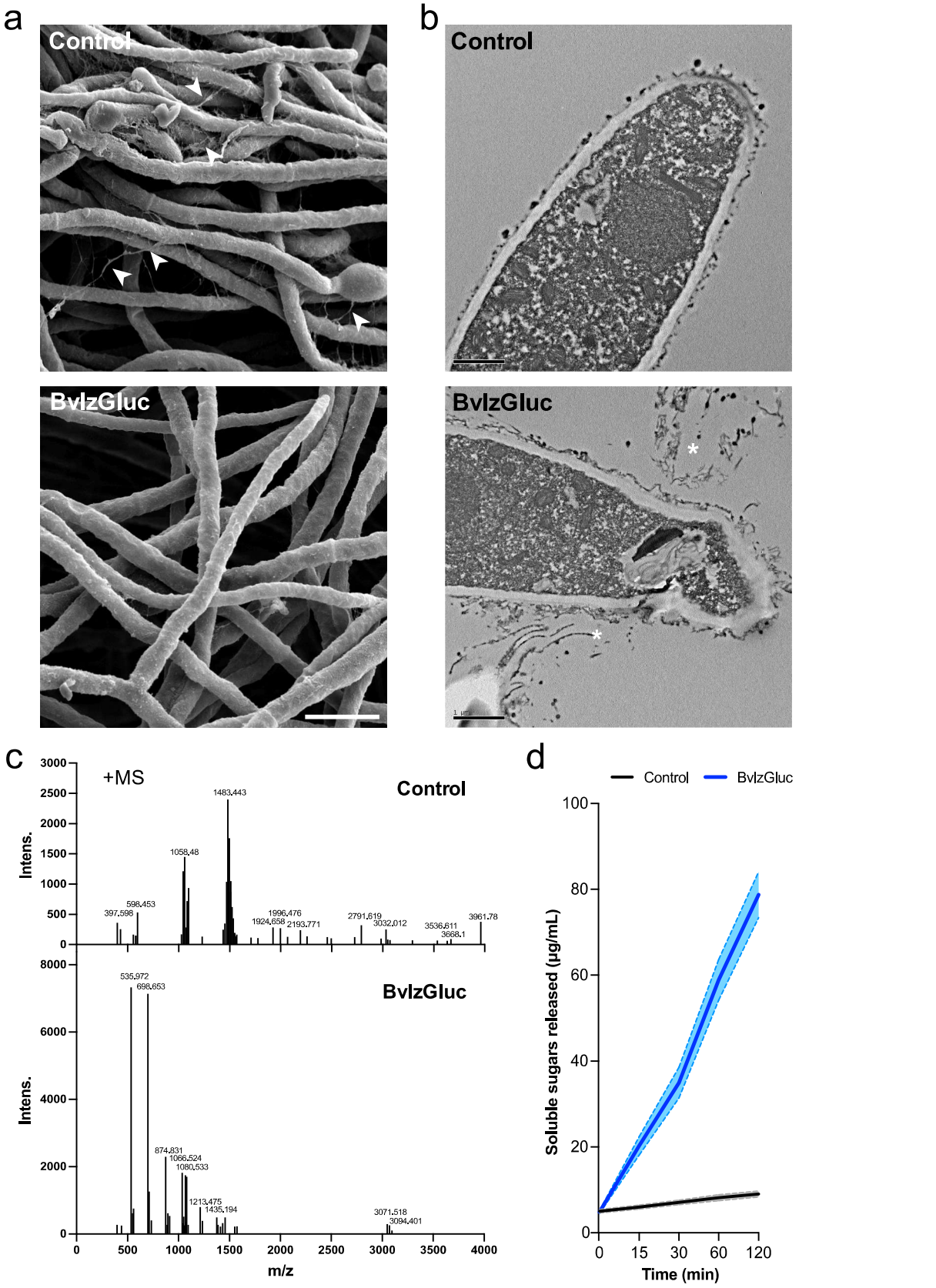

(caption on next page)

Fig. 2. Impact of BvlzGluc on *Botrytis cinerea* hyphal integrity. **a**. Scanning electron micrographs showing the *B. cinerea* extracellular matrix. BvlzGluc manifests remarkable activity on the extracellular matrix fibers that normally connect fungal hyphae (arrow heads). Upon treatment with BvlzGluc, these connective fibers were absent and coexisted with disruption of the hyphal network. The absence of these extracellular matrix components suggests that BvlzGluc interferes with key structural proteins or polysaccharides, further highlighting its potential as a targeted antifungal agent. Scale bar, 20 μm. **b**. Transmission electron micrographs showing clear morphological alterations in samples treated with BvlzGluc compared with untreated *B. cinerea* hyphae. Upon treatment with BvlzGluc, notable changes in the fungal cell wall structure were observed, particularly the release of fragments from the outer layer of the hyphal cell wall (white asterisk). Scale bar, 1 μm. **c**. MALDI-ToF mass spectrometry analysis of *Botrytis cinerea* cell wall extracts before and after treatment with BvlzGluc. Spectra were acquired in reflector positive ion mode (+MS). In Control samples, prominent high-molecular-weight peaks were detected, including signals centered around 1500 Da as well as larger species exceeding this range, consistent with the presence of long and partially branched β-glucan chains typical of the fungal cell wall. These peaks reflect the native polysaccharide architecture and suggest a population of incompletely fragmented glucan polymers. By contrast, treatment with BvlzGluc led to the complete disappearance of these high-molecular-weight signals and the emergence of low-molecular-weight peaks displaying regular mass differences of ~162 Da, which is characteristic of hexose (glucose) unit losses. This fragmentation pattern indicates that BvlzGluc catalyzes the *endo*-type hydrolysis of internal β-1,3-glycosidic bonds, generating oligosaccharide products with defined lengths. The observed shift in mass distribution provides functional confirmation of the enzyme's endo-β-1,3-glucanase activity, supports its specificity for linear β-glucans, and reinforces its proposed role as a noncanonical antifungal glucanase capable of destabilizing fungal cell wall polysaccharides. **d**. Time-course release of soluble carbohydrates from purified *Botrytis cinerea* cell wall material incubated with BvlzGluc (0.5 μM) or buffer control. Soluble sugars were quantified by the phenol–sulfuric acid assay and expressed as glucose equivalents (μg mL^{-1}). BvlzGluc induced a progressive and significant increase in solubilized material over 120 min, whereas control reactions showed minimal spontaneous hydrolysis.

3. Results and discussion

3.1. BvlzGluc reduces Botrytis spore germination and induces severe hyphal malformation

To identify protein determinants involved in the fungicidal activity of *B. velezensis* CECT 8237, a genomic library was constructed into the fosmid pCC2FOS™. A total of 400 clones were isolated, achieving full genome coverage of *Bacillus* at a depth of 4×. Compared with those from untreated plants or those treated with H_2O_2, cell-free supernatants from 12 different clones of the genome library induced a significant ROS response in response to *B. cinerea* spore suspensions (Supplementary Fig. 1). Positive clones were sequenced and analyzed to identify secreted extracellular proteins with potential fungicidal properties. This analysis considered the search for signal peptides, the absence of transmembrane domains, and extracellular localization. The obtained sequences were also compared with known databases to pinpoint specific genes or gene clusters responsible for antifungal activity (Supplementary Table 1). One of the fosmids contained a genomic fragment with the locus BAMY6639_07685 that met all the aforementioned analysis criteria. The deduced amino acid sequence (GenBank acc. no. WP_060674061) annotated as a hypothetical protein was selected as a candidate for further analysis. The sequence of this protein shares significant homology with that of glycoside hydrolases, which are enzymes known for their role in the hydrolysis of glycosidic bonds, which was a reason to tentatively designate it as BvlzGluc to reflect its putative glucosidase activity.

The biological effects of BvlzGluc on *Botrytis cinerea*, specifically on fungal spore germination, were studied. The protein was heterogeneously expressed in *E. coli* and purified to homogeneity before further experiments were performed. The protein strongly inhibited the germination of fungal spores that produced abnormally short, twisted germ tubes with minimal elongation (Fig. 1a). Eventually, some spores could germinate but still produced significantly fewer germ tubes (Fig. 1b). Untreated spores (Fig. 1a, inset) presented normal and extended germ tubes, indicating healthy fungal growth.

In addition, the external application of the protein to mature hyphae caused severe morphological deformations consisting of significant hyphal shortening accompanied by an increase in branching and pronounced vacuolization (Fig. 1c). This structural disruption suggested that the protein interferes with the normal growth and organization of fungal hyphae, resulting in abnormal cellular processes and compromising the overall integrity of the fungal network [34,35].

The inhibition of fungal spore germination triggered by bacterial β-glucanase has been previously described in *B. subtilis* CW14 against *Aspergillus ochraceus* [36] and *B. velezensis* CE [25]. These findings suggest that the inhibitory activity of BvlzGluc may share mechanistic similarities with that of other β-glucanases in targeting fungal pathogens by disrupting spore development and germination processes, further highlighting its potential as an antifungal agent.

3.2. BvlzGluc disrupts the outer layer of the fungal cell wall

A possible explanation for the morphological alterations observed in hyphae is a disruptive effect on fungal cell surfaces [37,38]. Scanning electron microscopy revealed the presence of an extracellular matrix surrounding the hyphae, normally forming an interconnected network (Fig. 2a, top), which appeared less evident after treatment with BvlzGluc (Fig. 2a, bottom; representative alterations indicated with arrows). This extracellular matrix is common in many fungi, both filamentous and non-filamentous, and plays a role in maintaining structural cohesion and communication between hyphae [39,40]. Transmission electron microscopy of thin sections of fungal hyphae showed areas where cell wall material seemed to be released from the structure (Fig. 2b, bottom, arrows), whereas no such features were detected in the control treated with protein buffer (Fig. 2b, top). These observations are consistent with BvlzGluc affecting the outer layer of the cell wall and the extracellular matrix that links hyphae, which may weaken the structural integrity of the fungal network and contribute to its antifungal effect [39,40].

To verify the specificity of the protein toward components of the fungal cell wall and extracellular matrix, purified cell wall fractions were incubated with BvlzGluc and analyzed by mass spectrometry (Fig. 2c). In the chromatograms of untreated hyphae, signals corresponding to high-molecular-weight polysaccharide chains were detected, as expected for intact fungal cell walls, together with weak and poorly defined peaks in the 1000–1500 *m/z* range. These minor signals most likely reflect partial degradation of β-glucan during the purification and handling steps, as reported for other preparations of complex polysaccharides.

By contrast, spectra obtained after incubation with BvlzGluc showed a marked reduction in high-molecular-weight species and the appearance of more abundant and better-defined peaks in the 1000–1500 m/z region (Fig. 2c). Importantly, several of these signals followed increments of approximately 162 Da, which corresponds to the mass of a glucose unit and is widely recognized as a diagnostic feature of β-glucan oligomers (Supplementary table 3) [41]. The presence of these structured series of peaks, absent or only marginally visible in control samples, is consistent with the release of soluble glucan fragments as a consequence of enzymatic hydrolysis.

The increased intensity and organization of these oligomeric ladders in treated samples therefore provide molecular-level evidence that BvlzGluc cleaves glycosidic bonds within fungal β-glucans, converting high-molecular-weight polysaccharides into shorter oligomeric products. This activity is consistent with the proposed role of BvlzGluc as a β-glucanase and suggests a mechanism by which the enzyme may weaken or remodel the structural matrix of the fungal cell wall, thereby contributing to its antifungal effect [42,43]. It should be noted that, for

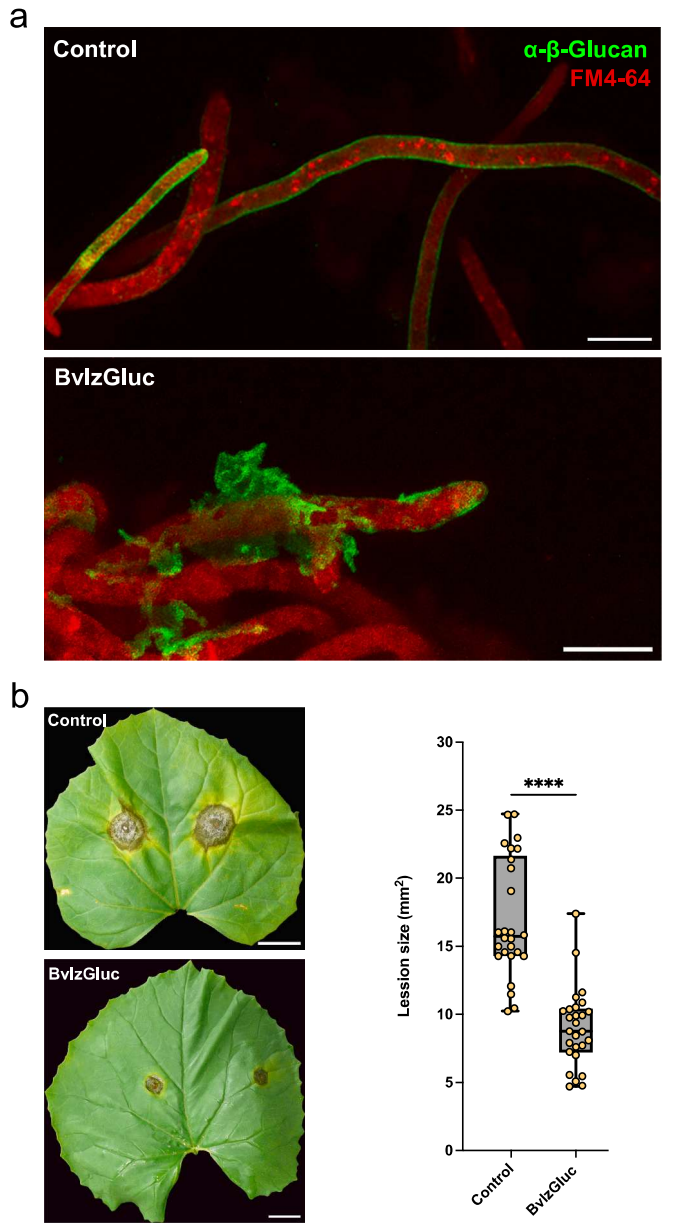

Fig. 3. Effect of BvlzGluc on *Botrytis cinerea* infection in plants. **a**. Immunocytochemical analysis using an anti-fungal monoclonal primary antibody and a GFP-conjugated anti-rabbit secondary antibody demonstrated the normal distribution of β-glucans in *Botrytis cinerea* hyphae. In the control samples, the β-glucans formed a regular, continuous, and uniform layer within the cell wall, which is crucial for maintaining cell wall integrity and structural support in the fungus. However, upon treatment with BvlzGluc, significant disruptions in the β-glucan layer were observed. These discontinuities suggest that BvlzGluc interferes with the synthesis or maintenance of β-glucans, likely weakening the fungal cell wall and increasing its vulnerability to external stress. **b**. Lesion size triggered by *B. cinerea* on melon leaves after 72 hpi was reduced by 80 % upon treatment with BvlzGluc. The whisker plot shows all the measurements (orange dots), medians (black line), and minimum and maximum values (whisker ends). The datasets did not pass the Shapiro–Wilk test for normality ($P > 0.05$) and were compared using a nonparametric two-tailed Mann–Whitney test, with quadruple asterisks indicating significant differences at $P < 0.0001$.

the SEM and TEM analyses, we intentionally focused on hyphal regions that were not yet fully collapsed, so that the outer wall and extracellular fibrillar matrix could still be resolved. In the most severely damaged areas, these structures were too disrupted to be analyzed reliably. This explains why the ultrastructural images in Fig. 2 appear less deformed than the whole-hypha phenotypes observed in Fig. 1, while both sets of images represent complementary manifestations of the same BvlzGluc-induced damage.

To complement the mass spectrometry analysis and provide a quantitative assessment of cell wall degradation, the release of soluble sugars from purified fungal cell walls incubated with BvlzGluc was measured, control reactions displayed minimal solubilization over the 120 min incubation period, consistent with limited spontaneous hydrolysis. In contrast, treatment with BvlzGluc resulted in a clear and time-dependent increase in soluble carbohydrate content, reaching approximately 80 μg mL^{-1} of glucose equivalents at 120 min (Fig. 2d). These data indicate that BvlzGluc promotes solubilization of fungal cell wall polysaccharides, providing quantitative evidence of enzymatic hydrolysis that fully aligns with the oligomeric fragmentation pattern observed by mass spectrometry (Fig. 2c).

3.3. *BvlzGluc degrades fungal β-glucan, weakening cell wall integrity and reducing Botrytis cinerea virulence*

The effect of BvlzGluc on *B. cinerea* was visualized in vivo via immunocytochemistry using a fungal anti-β-glucan-specific antibody. In the control sample, the β-glucan layer was clearly detected on the outermost region of the fungal cell wall. The fluorescence signal was continuous throughout the entire hypha, with higher intensity at the hyphal apex, indicating an intact and organized β-glucan layer structure. However, when the hyphae were treated with the protein BvlzGluc, the fluorescent signal associated with the β-glucan layer was no longer visible as a continuous structure. Fragments of the β-glucan layer adhered to the outer region of the cell wall, and additional β-glucan fragments were scattered randomly along the hyphae (Fig. 3a). This observation indicates that the protein has a clear impact on the β-glucan layer, consistent with degradation and alterations in the structural organization of the cell wall, which may affect rigidity and flexibility, both relevant for fungal growth and infection [36,44,45]. This degradation likely weakens the structural integrity of the cell wall, potentially reducing the ability of the fungus to grow and infect. To assess the biological impact of removing the β-glucan layer, the virulence of *Botrytis* was evaluated by measuring the lesion area on melon plant leaves. The lesion area in the presence of BvlzGluc was significantly smaller than that in the untreated control (Fig. 3b). On the basis of these findings, we propose that degradation of the outer β-glucan layer may contribute to reduced Botrytis virulence by i) destabilizing fungal integrity and ii) potentially facilitating the activation of plant immune responses through exposure of inner cell wall components [46,47].

3.4. *Concentration-dependent aggregation of BvlzGluc reduces its efficacy*

BvlzGluc purified in vitro yielded a distinctive band of 15 kDa (Fig. 4a), which was consistent with the estimated molecular weight at a concentration of 0.5 μM. However, as the protein concentration increased to 1.5 and 2.5 μM, the 15 kDa band was replaced by a higher molecular weight band of 50 kDa. Interestingly, the decreased efficacy of the biological functionality of the protein against *Botrytis* was correlated with the increase in protein concentration (Fig. 4b). This inverse relationship is consistent with high protein concentration promoting the formation of non-functional assemblies. Consistent with this interpretation, TEM analysis of negatively stained samples revealed clear aggregates at elevated concentrations that were absent at 0.5 μM (Fig. 4c). These aggregates provide direct visual evidence of concentration-dependent self-association under native conditions, providing a plausible explanation for the reduced biological activity of the protein at higher concentrations. Previous studies have indicated that β-glucanases can aggregate under specific conditions, resulting in larger molecular weight complexes that diminish enzymatic efficiency [8,48].

The resistance of the purified protein to different physicochemical conditions, such as temperature and pH, was further tested. The enzyme

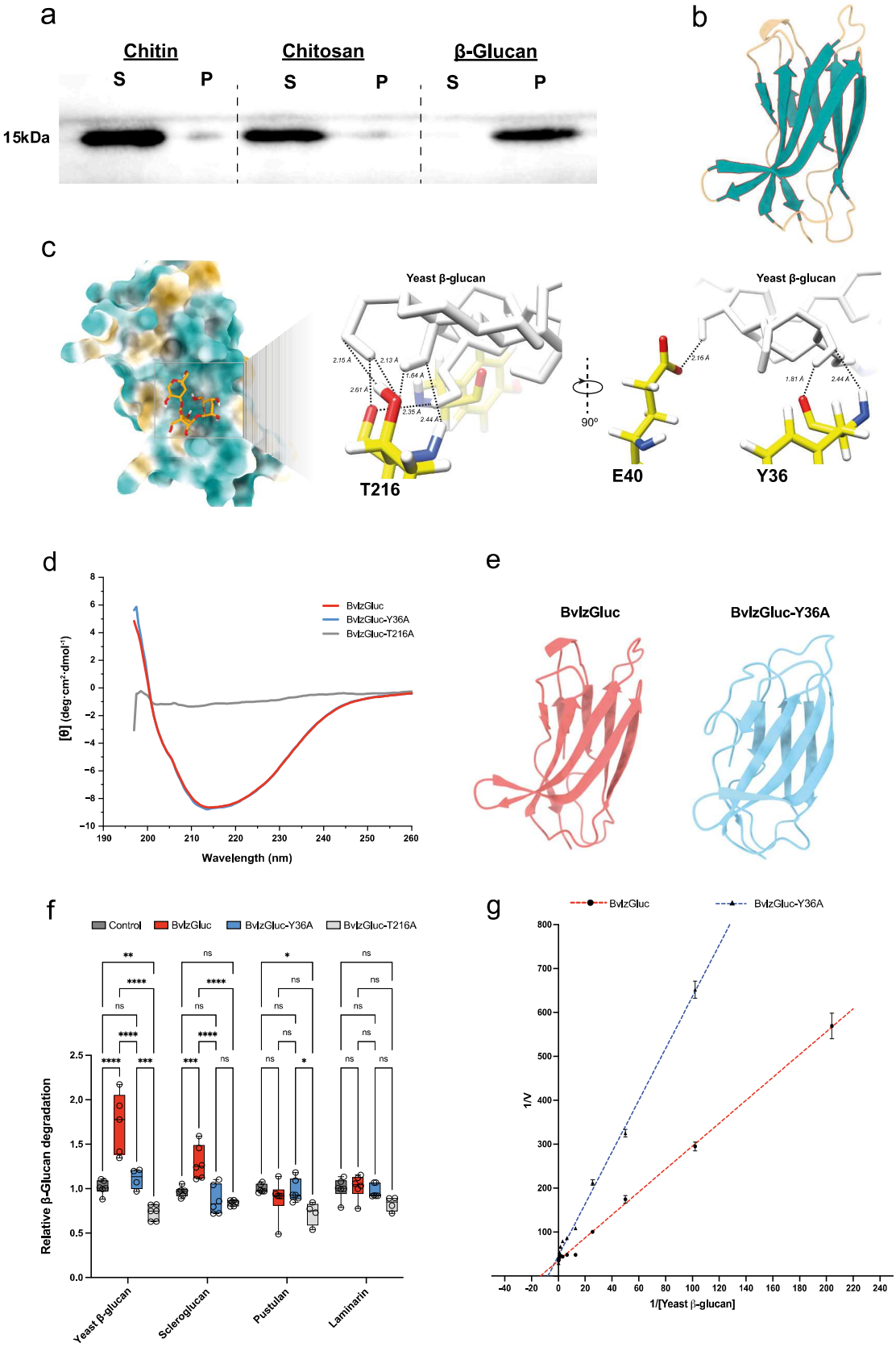

(caption on next page)

Fig. 4. Purification and characterization of BvlzGluc. **a**. SDS–PAGE analysis revealed an unexpected phenomenon during purification: while the protein was successfully purified (15 kDa), increasing its concentration resulted in the appearance of a band corresponding to an entity with a molecular weight higher than expected (50 kDa). **b**. In terms of antimicrobial activity, BvlzGluc has the ability to induce the formation of reactive oxygen species (ROS) in *Botrytis cinerea*, but this activity relies on the protein concentration. At low concentrations, the protein effectively triggered an oxidative burst, contributing to its potential role as an antimicrobial agent. However, as the concentration increased, its ability to induce ROS generation decreased, leading to a complete loss of activity at higher concentrations. **c**. Aggregation of BvlzGluc at high concentrations was confirmed, supporting the hypothesis that a lack of activity is linked to protein aggregation. This behavior could be due to the tendency of proteins to self-associate at relatively high concentrations, resulting in the formation of inactive aggregates. **d**. Physicochemical characterization of BvlzGluc revealed important details about its stability and activity under various environmental conditions. The optimal temperature for its enzymatic activity was established at 40 °C, indicating that BvlzGluc can function efficiently at relatively high temperatures, making it suitable for applications with thermal stability requirements. Additionally, the optimal pH was 7, suggesting that BvlzGluc performs best under neutral conditions.

displayed maximal activity at approximately 40 °C (Fig. 4d), which indicates that it retains activity at moderately elevated temperatures [49,50]. Additionally, the enzyme was determined to operate most effectively under neutral conditions (pH 7) (Fig. 4e). This is a common feature of many β-glucanases in certain plant tissues that are crucial for plant growth and defense against pathogens, facilitating the degradation of pathogen cell walls [51,52]. The combination of tolerance to moderately high temperatures and a neutral pH optimum is compatible with the enzyme functioning in ecological or physiological niches where these conditions prevail, such as soil or plant-associated environments with fluctuating temperatures and pH levels [44,53].

3.5. *BvlzGluc specifically targets β-glucan*

To specifically determine the target of this protein, separate suspensions of each cell wall component (β-glucans, chitin, or chitosan) were prepared and incubated with the protein. After the incubation period, the samples were centrifuged to separate the pellet (containing nondegraded or insoluble material) from the supernatant (containing soluble or degraded components). Western blot analysis using anti-His tag antibodies was performed to identify whether the protein bound to or degraded any of the cell wall components found in either fraction [29,54]. In the presence of both chitin and chitosan, the protein was detected in the supernatant (Fig. 5a). In addition, confocal microscopy analysis with specific staining of chitin and chitosan revealed undistinguishable fluorescence signals in untreated hyphae and hyphae treated with the protein (Supplementary fig. 2). These observations indicate that BvlzGluc does not show detectable direct interaction with these two major cell wall components under our experimental conditions [36].

However, in the presence of yeast β-glucan, the protein was found in the pellet, indicating that the protein specifically binds yeast β-glucan (Fig. 5a). Yeast β-glucan is widely used as a reference β-1,3-glucan substrate in enzymatic studies, and therefore provides an appropriate standard for assessing the activity of BvlzGluc [7,36]. This biochemical affinity of the protein for yeast β-glucans, along with the ultrastructural changes in the outer layers of the cell wall (Fig. 2) and fragmentation of the polymers (Fig. 2c, mass spectrometry analysis), are compelling results that support the specificity of the protein for this chemical fraction of the fungal cell wall. The mass spectrometry analysis reflects β-1,3-glucan hydrolysis from the native cell wall; although the experiment was performed on endogenous β-glucan rather than on a purified commercial preparation, the fragmentation profile is consistent with *endo*-β-1,3 cleavage and is further supported by the enzyme's activity on laminarin, scleroglucan and pustulan. The precipitation observed with β-glucans suggested that the protein's action might involve structural changes or degradation of the β-glucan matrix, leading to the formation of insoluble complexes.

3.6. *Structural and mechanistic insights into BvlzGluc*

BvlzGluc features a jelly roll structure, this architecture is composed of several antiparallel beta-sheets that contribute to its thermal stability and function, particularly through the formation of β-strands into two twisted antiparallel β-sheets, which creates a concave and convex surface (Fig. 5b). These surfaces assist in stabilizing interactions such as hydrogen bonding and hydrophobic contacts, which are crucial for maintaining structural integrity at elevated temperatures [55,56].

Molecular docking of the protein with yeast β-glucan was carried out to determine the potential binding site and to identify the putative residues involved in the interaction, but not to predict a definitive catalytic pose. The analysis predicted 10 clusters of putative binding sites distributed across 16 different regions of the protein. The most energetically favorable binding site, ΔG = -8.3 kcal mol-1, was located within the core of the protein. The binding of yeast β-glucan to a protein mostly relies on the establishment of nine hydrogen bonds with residues Y36, E40 and T216. Distances to those residues were 1.81 Å, 2.44 Å, 2.16 Å, 2.15 Å, 2.61 Å, 2.13 Å, 2.35 Å, 2.44 Å and 1.64 Å, respectively (Fig. 5c). Interestingly, a structurally equivalent tyrosine residue (Y36) has been described in the potato endo-β-1,3-glucanase GLUB20–2, where it appears to restrict the accommodation of branched polysaccharides within the catalytic cleft [57].

These residues had not previously been associated with catalytic activity or structural conservation in glucanases, but the docking results suggested they might establish direct contacts with β-glucan. Therefore, to validate whether these residues participate in substrate interaction, site-directed mutagenesis was carried out, generating the Y36A and T216A variants. The secondary structure of these variants was assessed by far-UV circular dichroism (CD) and compared to that of the wild-type protein. The latter displayed a spectrum typical of β-sheet-rich proteins, with a broad negative band near 217 nm and a maximum around 195 nm (Fig. 5d), consistent with a predominantly β-structured fold.

The Y36A variant showed a nearly identical CD profile, indicating that this mutation does not significantly alter the global secondary structure. In contrast, the T216A variant exhibited a markedly different CD spectrum, lacking the defined β-sheet signature and showing instead a strong negative band near 200 nm, which is characteristic of a partially or fully unfolded conformation. These results suggest that the T216A mutation induces major structural destabilization, and therefore its enzymatic phenotype cannot be directly attributed to a specific functional role. This observation was further supported by structural modeling, which predicted highly similar 3D folds for the wild-type and Y36A proteins (Fig. 5e). In the wild-type model, residue Y36 is oriented toward the substrate-binding groove, in proximity to the predicted β-glucan docking site. Its substitution with alanine removes a bulky, polar side chain from this region, potentially disrupting substrate positioning or stabilization.

To functionally characterize the BvlzGluc protein and determine its substrate specificity, we tested its activity against a panel of structurally diverse polysaccharides: yeast β-glucan, scleroglucan, pustulan, and laminarin. BvlzGluc exhibited markedly higher activity against yeast β-glucan, while its activity on the other polysaccharides was significantly lower and near background levels (Fig. 5f). This substrate preference indicates that BvlzGluc primarily targets linear β-1,3-glucans and exhibits low tolerance to β-1,6-branching. The lack of activity on pustulan, a β-1,6-linked homopolysaccharide, excludes β-1,6-glucanase activity. The reduced activity on scleroglucan and laminarin, which contain both β-1,3 and β-1,6 linkages, further suggests that branching interferes with substrate recognition or hydrolysis. This functional profile is typical of an *endo*-β-1,3-glucanase, these enzymes hydrolyze

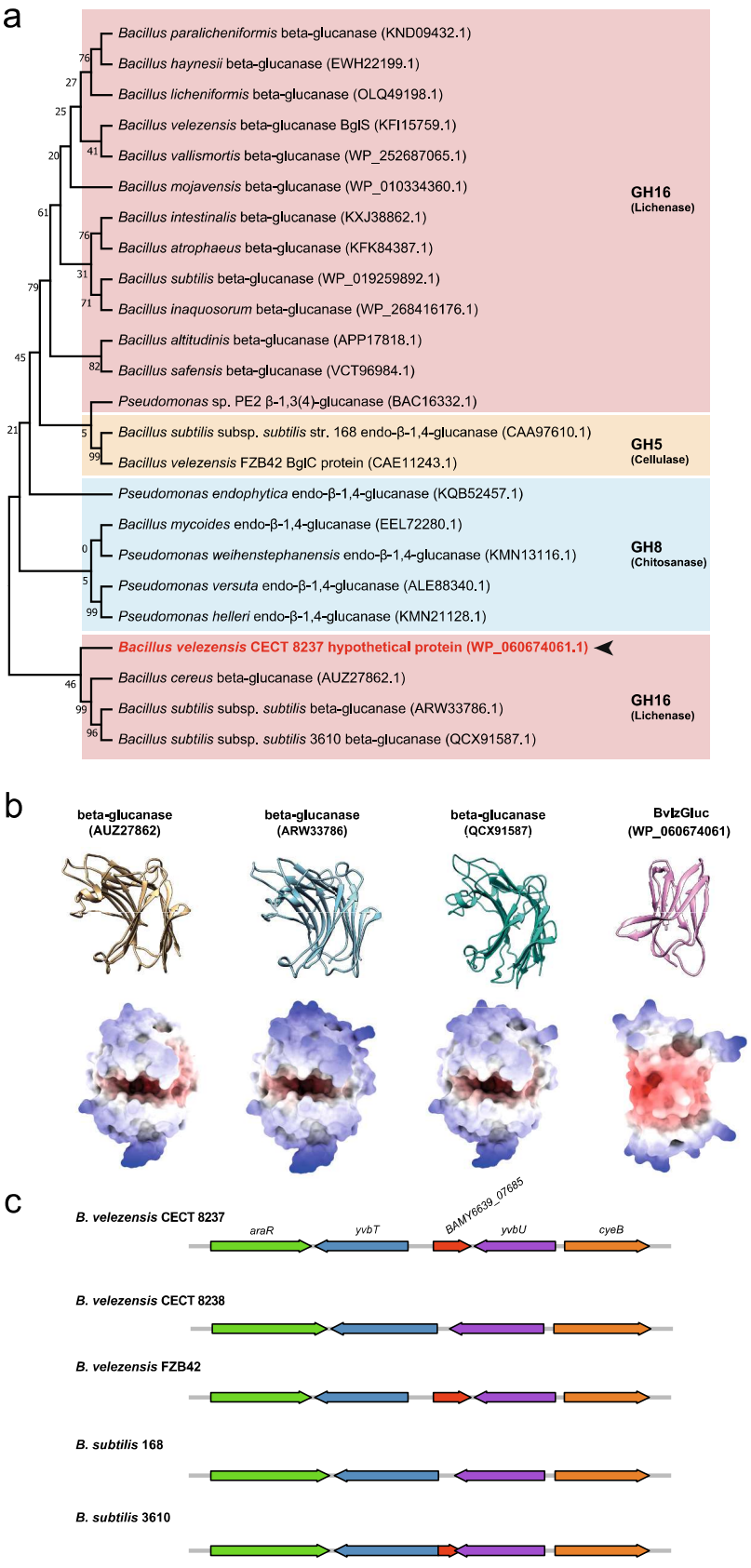

(caption on next page)

Fig. 5. Functional analysis of BvlzGluc. **a**. Binding analysis of different carbohydrates typically present in the fungal cell wall. Through the sedimentation assay, BvlzGluc was consistently found in the pellet along with β-glucan, indicating a specific binding interaction between the enzyme and this polysaccharide. This finding suggests that BvlzGluc has a high affinity for β-glucan, likely playing a crucial role in its degradation or modification. **b**. Predicted 3D structure of BvlzGluc showing the characteristic β-jelly-roll fold typical of GH16 β-glucanases, composed of two curved antiparallel β-sheets forming a β-sandwich architecture. The conservation of this core structural scaffold supports its placement within the GH16 family despite its pronounced sequence divergence. **c**. Molecular docking between the yeast β-glucan molecule and BvlzGluc. The proposed binding site is formed by residues Y36, E40 and T216 forming nine hydrogen bonds; the measured distances between yeast β-glucan and the side chains of these residues were 1.81 Å, 2.44 Å, 2.16 Å, 2.15 Å, 2.61 Å, 2.13 Å, 2.35 Å, 2.44 Å and 1.64 Å, respectively. **d**. Circular dichroism (CD) spectra of the wild-type, Y36A, and T216A proteins. While the wild-type and Y36A exhibit overlapping spectra consistent with a β-sheet-rich fold, the T216A mutant displays a spectrum typical of unfolded or misfolded proteins. **e**. Predicted 3D structures of wild-type BvlzGluc and the Y36A variant. Structural modeling shows that both proteins adopt a similar global fold. In the wild-type model, residue Y36 is positioned near the putative substrate-binding groove, suggesting a possible role in substrate stabilization or positioning. Replacement with alanine does not affect the overall conformation but removes a bulky, polar side chain from the binding region, potentially impairing catalytic function without disrupting structural integrity. **f**. Substrate specificity profile of BvlzGluc against structurally distinct β-glucans. The enzyme was tested for hydrolytic activity on a panel of polysaccharides including yeast β-glucan, laminarin, pustulan and scleroglucan. Significant activity was only observed for yeast β-glucan, indicating that BvlzGluc specifically targets linear β-1,3-glucans and does not efficiently hydrolyze β-1,6- or β-1,3/1,4-linked substrates. This pattern supports its functional classification as a noncanonical endo-β-1,3-glucanase. **g**. Lineweaver–Burk plots comparing the kinetic behavior of wild-type BvlzGluc and the Y36A variant. The reaction velocities were determined at increasing concentrations of yeast β-glucan and plotted as double reciprocal curves to derive kinetic parameters. The Y36A mutant exhibited a steeper slope and a higher Y-intercept compared to the wild-type enzyme, indicating a reduction in catalytic efficiency (Vmax) while maintaining a similar X-intercept, which corresponds to the apparent Km. These results suggest that the mutation at position Y36 predominantly affects the catalytic turnover rate rather than substrate binding affinity. The kinetic profile of the wild-type enzyme fits well with a Michaelis–Menten model and confirms its classification as an endo-β-1,3-glucanase, while the altered kinetics of Y36A highlight the functional relevance of this residue in enzymatic catalysis.

internal β-1,3-glycosidic bonds, a key component of fungal cell walls. Accordingly, several endo-β-1,3-glucanases have been reported to possess antifungal activity, as they compromise fungal cell wall integrity and lead to cell lysis [57,58]. In rhizosphere bacteria such as *Bacillus subtilis*, endo-β-1,3-glucanases have been described as secreted effectors involved in microbial competition and biocontrol of phytopathogenic fungi [59].

Functional analysis of the Y36A variant showed reduced activity on yeast β-glucan relative to the wild-type protein, while activity on the other polysaccharides remained unchanged (Fig. 5f). This supports the hypothesis that Y36 participates in substrate recognition, particularly for linear β-1,3-glucans, as predicted by molecular docking. This approach, combining molecular docking and functional validation, has proven effective in other GH families to map key binding-site residues that are not necessarily conserved [60,61].

Kinetic analysis of the wild-type enzyme revealed a typical Michaelis–Menten behavior, (Supplementary fig. 3). Based on this profile, a Lineweaver–Burk (double-reciprocal) plot was generated (Fig. 5g) to estimate the enzymatic parameters. The resulting values were a Km of 47.92 μM and a Vmax of 0.02621 μmol/min. These kinetic parameters are consistent with those reported for other β-1,3-glucanases of bacterial or fungal origin. For instance, β-glucanases from *Trichoderma koningii* and *Paenibacillus* species acting on yeast β-glucan typically display K_m values in the range of 30–300 μM, depending on substrate solubility and assay conditions [62]. In this context, the relatively low K_m observed for our enzyme suggests a strong affinity for the β-glucan substrate. However, the modest V_{max} observed may reflect the structural complexity or limited solubility of yeast-derived β-glucan, which is known to influence turnover rates in similar assays [63,64]. Overall, the catalytic profile of the wild-type protein is in line with glucanases reported to act on fungal cell wall components and supports its potential role in antifungal activity.

Among the variants, only Y36A retained a native-like fold and was suitable for kinetic analysis, as confirmed by its CD spectrum. This mutant exhibited an increased slope (K_m/V_{max}) and a higher Y-intercept compared to the wild type, indicating a reduction in catalytic efficiency, primarily due to a lower V_{max}. The X-intercepts were similar, suggesting that substrate affinity (K_m) was not substantially affected, and that the mutation predominantly impairs the catalytic turnover.

The T216A variant was excluded from kinetic comparisons due to its unfolded conformation, as evidenced by its altered CD spectrum.

3.7. *BvlzGluc is a noncanonical β-glucanase*

The phylogenetic analysis of the amino acid sequence revealed that BvlzGluc clusters with other β-glucanases from *B. subtilis* and *B. cereus* (Fig. 6a; Supplementary table 2); despite this, it exhibited notable differences from other *B. velezensis* proteins previously described as β-glucanases [65,66]. This observation indicates that, although the protein shares evolutionary ancestry with β-glucanases from related *Bacillus* species, it follows a somewhat different phylogenetic trajectory from the more commonly recognized β-glucanases in *B. velezensis*. The fact that BvlzGluc clusters more closely with proteins from *B. subtilis* and *B. cereus* is consistent with a conserved evolutionary lineage between these species and may reflect functional similarity or shared ecological roles in these bacterial species.

Moreover, the placement of this protein within glycoside hydrolase family 16 (GH16) is of particular interest. This classification is further supported by HMMER annotation, which identified a GH16 domain with highly significant scores. The GH16 family is known for containing enzymes that primarily hydrolyze β-glycosidic bonds in polysaccharides, particularly β-glucans such as lichenin [67,68]. To illustrate the degree of sequence divergence within GH16 enzymes, we compared BvlzGluc with the crystallized GH16 *endo*-β-1,3-1,4-glucanase from *Bacillus licheniformis* (PDB 1GBG) (Supplementary Fig. 4). Although the overall identity between both proteins is low (12 %) and BvlzGluc lacks the canonical EIDIEF motif present in the *B. licheniformis* enzyme, such variability is well documented within the GH16 family, which encompasses highly divergent sequences that nonetheless retain a conserved β-jelly-roll structural core [69,70]. Accordingly, this comparison highlights the atypical nature of BvlzGluc within GH16 rather than contradicting its classification. The assignment to GH16 is supported by HMMER annotation using CAZy-derived GH16 profiles, phylogenetic clustering with GH16 β-glucanases from *Bacillus* species, and the conservation of the characteristic GH16 fold in the predicted 3D structure [71].

This motif is often critical for the catalytic function of many β-glucanases, implying that the protein might employ a different mechanism for substrate recognition or catalysis [9,71].

The jelly roll structure of BvlzGluc is a distinctive characteristic of the GH16 family of glucan hydrolases [72,73]. Together with its β-barrel-like architecture, the jelly roll fold is also characterized by the presence of a deep groove on the protein's surface, which acts as the substrate-binding site (Fig. 6b) [47,48]. Interestingly, this groove is absent in BvlzGluc but apparently does not affect its enzymatic functionality; therefore, BvlzGluc may utilize alternative mechanisms for substrate binding or interaction, possibly relying on different surface properties or conformational flexibility to achieve its biological role. This structural divergence from canonical β-glucanases suggests that BvlzGluc may exhibit distinct biochemical or ecological features within

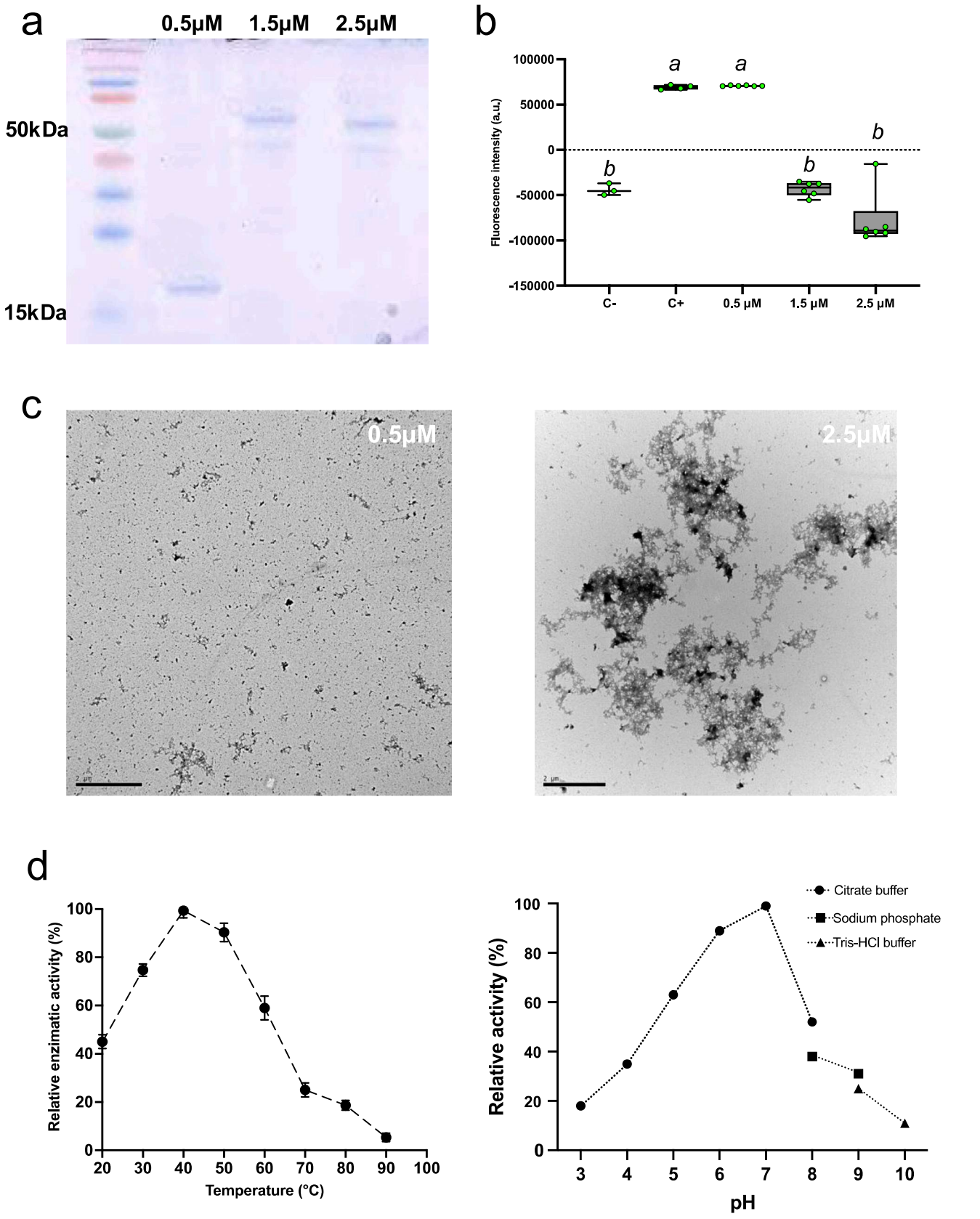

(caption on next page)

Fig. 6. Phylogenetic and structural analysis of BvlzGluc (WP_060674061) and its structural comparison with β-glucanases from other phylogenetically related bacterial strains. **a**. In the phylogenetic analysis, BvlzGluc tended to group with β-glucanases from *B. cereus* and *B. subtilis* rather than with β-glucanases from other *B. velezensis* strains. This unexpected grouping suggests that BvlzGluc may have functional or structural characteristics more similar to those of the β-glucanases of these species. Further analysis revealed that BvlzGluc likely belongs to glycoside hydrolase family 16 (GH16), which is known for its ability to degrade complex polysaccharides containing mixed-linkage glucans, such as β-1,3- and β-1,4-glucans. Enzymes from this family specialize in degrading structural polysaccharides present in plant and fungal cell walls, highlighting the potential role of BvlzGluc in targeting a broad range of substrates. The evolutionary divergence of BvlzGluc from other *B. velezensis* β-glucanases could reflect functional adaptations, possibly providing unique substrate specificities or modes of action within the GH16 family. **b**. Structural comparison of proteins within the same phylogenetic cluster revealed that despite their evolutionary alignment, the proteins presented notable structural differences. While they all share the conserved jelly roll fold, which is a common motif in many β-barrel proteins, BvlzGluc does not possess the deep groove typically associated with enzymatic activity. This absence suggests that although these proteins may be evolutionarily related, they might have diverged in specific functions. **c**. Analysis of the genetic context of the BvlzGluc-encoding gene *BAMY6639_07685* revealed interesting patterns of distribution among *Bacillus* species. This gene was identified in *B. velezensis* FZB42, the representative strain for the group, suggesting that it plays a significant role in the functional capabilities of this strain, potentially contributing to its specialized enzymatic activities. However, in *B. subtilis*, the gene was either completely absent or truncated, indicating a possible loss or modification of function during evolution.

its environmental context. It will be interesting in future work to determine whether these structural differences translate into specialized roles in polysaccharide degradation in specific niches.

A comparative gene cluster analysis was conducted to determine the genetic context of the BvlzGluc protein across different *Bacillus* strains. The gene clusters for *B. velezensis* CECT 8237, CECT 8238, FZB42, and *B. subtilis* 168 and 3610 presented a high degree of structural conservation, except for the BAMY6639_07685-encoding gene. This gene is complete and functional in *B. velezensis* CECT 8237 as well as in *B. velezensis* FZB42. However, it is absent in the strains *B. velezensis* CECT 8238 and *B. subtilis* 168. Interestingly, in *B. subtilis* 3610, the gene is annotated as a pseudogene, indicating that while remnants of the gene remain, it likely does not produce a functional protein (Fig. 6c). The absence or inactivation of this gene in some strains suggests potential evolutionary divergence related to specific functional requirements or ecological adaptations. In strains in which the gene is functional, such as *B. velezensis* CECT 8237 and FZB42, the presence of BvlzGluc could be associated with distinct metabolic pathways or environmental interactions that confer a selective advantage, particularly in terms of plant–microbe interactions or antifungal activity. In fact, comparative genomic analyses revealed that *B. velezensis* strains, including CECT 8237 and FZB42, share a core genome enriched in secondary metabolism genes, including key genes involved in plant–microbe interactions and antifungal activities [23,74]. In contrast, the lack of this gene or the lack of nonfunctional versions reflects evolutionary divergence, suggesting an adaptive response in which the gene becomes nonessential in particular ecological niches [22,75].

4. Conclusion

BvlzGluc is a β-glucanase enzyme produced by *Bacillus velezensis* CECT 8237 that shows high specificity toward β-1,3-glucans, including those forming the structural core of the *Botrytis cinerea* cell wall. Its enzymatic activity results in the fragmentation of these polysaccharides into lower-molecular-weight products, as demonstrated by mass spectrometry, and is associated with morphological alterations, impaired fungal development, and reduced virulence in planta. These findings are consistent with the activity of *endo*-β-1,3-glucanases and support the antifungal potential of this enzyme.

Our results indicate that BvlzGluc adopts a jelly roll fold typical of glycoside hydrolase family 16 (GH16), but lacks several conserved features commonly found in canonical members. Despite sharing the overall fold, it presents distinct structural traits, such as the absence of a classical catalytic groove and of conserved sequence motifs. Site-directed mutagenesis of residues Y36 and T216, predicted by molecular docking to participate in substrate interaction, revealed their importance in enzymatic function and protein folding, respectively. Altogether, these data suggest that BvlzGluc could represent a noncanonical enzyme within the GH16 family.

In addition, BvlzGluc displays stability under a range of pH and temperature conditions, and its relatively simple architecture could facilitate recombinant production. These properties, together with its substrate specificity and observed antifungal activity, suggest that BvlzGluc may hold potential for future biotechnological applications, particularly in the context of sustainable agriculture. However, further studies are needed to assess its performance under applied conditions and to explore the broader diversity and ecological functions of bacterial β-glucanases involved in microbial antagonism and biocontrol.

CRediT authorship contribution statement

D. Vela-Corcia: Writing – original draft, Investigation, Funding acquisition, Formal analysis, Conceptualization. **A. de Vicente:** Writing – review & editing. **A. Pérez-García:** Writing – review & editing. **D. Romero:** Writing – review & editing, Writing – original draft, Funding acquisition, Conceptualization.

Declaration of competing interest

The authors declare that they have no known competing financial interests or personal relationships that could have appeared to influence the work reported in this paper.

Acknowledgments

We thank Saray Morales Rojas for its technical support; Alicia Esteban and David Navas from the IHSM and SCAI microscopy units, respectively, for their technical support in confocal microscopy; and Mercedes Martín Rufián from the Proteomic Unit from the SCAI-UMA for their technical suggestions.

This work was partially supported by grants from the ERC Starting Grant (BacBio 637971), Plan Nacional de I + D + I of the Ministerio de Economía y Competitividad (PID2019-107724GB-I00, PID2022-141664NB-I00), research contract 8.06/60.4086 with KOPPERT B.V. (The Netherlands), and Proyecto Jóvenes Investigadores from the Plan Propio de Universidad de Málaga (B1-2021_34), with D.V.C. as the Principal Investigator. D.V.C. is funded by the Incorporación de Doctores PAIDI from Junta de Andalucía program (DOC_00266).

Appendix A. Supplementary data

Supplementary data to this article can be found online at https://doi.org/10.1016/j.ijbiomac.2026.150106.

Data availability

Data will be made available on request.

References

[1] S.M. Bowman, S.J. Free, The structure and synthesis of the fungal cell wall, BioEssays 28 (2006) 799–808, https://doi.org/10.1002/bies.20441.

[2] F.M. Klis, P. Mol, K. Hellingwerf, S. Brul, Dynamics of cell wall structure in Saccharomyces cerevisiae, FEMS Microbiol. Rev. 26 (2002) 239–256, https://doi.org/10.1111/j.1574-6976.2002.tb00613.x.

[3] G. Lesage, H. Bussey, Cell Wall assembly in Saccharomyces cerevisiae, Microbiol. Mol. Biol. Rev. 70 (2006) 317–343, https://doi.org/10.1128/mmbr.00038-05.

[4] J.P. Latgé, The cell wall: a carbohydrate armour for the fungal cell, Mol. Microbiol. 66 (2007) 279–290, https://doi.org/10.1111/j.1365-2958.2007.05872.x.

[5] J. Ruiz-Herrera, L. Ortiz-Castellanos, Cell wall glucans of fungi. A review, Cell Surface 5 (2019), https://doi.org/10.1016/j.tcsw.2019.100022.

[6] G. Camilli, G. Tabouret, J. Quintin, The complexity of fungal β-glucan in health and disease: effects on the mononuclear phagocyte system, Front. Immunol. 9 (2018), https://doi.org/10.3389/fimmu.2018.00673.

[7] V.N. Monteiro, C.J. Ulhoa, Biochemical characterization of a β-1,3-glucanase from Trichoderma koningii induced by cell wall of Rhizoctonia solani, Curr. Microbiol. 52 (2006) 92–96, https://doi.org/10.1007/s00284-005-0090-2.

[8] K.R.S. Celestino, R.B. Cunha, C.R. Felix, Characterization of a β-glucanase produced by Rhizopus microsporus var. microsporus, and its potential for application in the brewing industry, BMC Biochem. 7 (2006), https://doi.org/10.1186/1471-2091-7-23.

[9] G.P. Furtado, L.F. Ribeiro, C.R. Santos, C.C. Tonoli, A.R. De Souza, R.R. Oliveira, M. T. Murakami, R.J. Ward, Biochemical and structural characterization of a β-1,3-1,4-glucanase from Bacillus subtilis 168, Process Biochem. 46 (2011) 1202–1206, https://doi.org/10.1016/j.procbio.2011.01.037.

[10] J.W. Cao, Q. Deng, D.Y. Gao, B. He, S.J. Yin, L.C. Qian, J.K. Wang, Q. Wang, A novel bifunctional glucanase exhibiting high production of glucose and cellobiose from rumen bacterium, Int. J. Biol. Macromol. 173 (2021) 136–145, https://doi.org/10.1016/j.ijbiomac.2021.01.113.

[11] B. Henrissat, G. Daviest, Structural and Sequence-based Classification of Glycoside Hydrolases. http://biomednet.com/elecref/O959440XO0700637, 1997.

[12] S.N.N. Zondo, L. Mohase, V.L. Tolmay, M.S. Mafa, Functional characterisation of cell wall-associated β-glucanases and peroxidase induced during wheat-Diuraphis noxia interactions, Biologia (Bratisl) 79 (2024) 2873–2890, https://doi.org/10.1007/s11756-024-01734-1.

[13] V. Lombard, H. Golaconda Ramulu, E. Drula, P.M. Coutinho, B. Henrissat, The carbohydrate-active enzymes database (CAZy) in 2013, Nucleic Acids Res. 42 (2014), https://doi.org/10.1093/nar/gkt1178.

[14] L.K. Edison, P.K. Satheeshkumar, N.S. Pradeep, Industrial production and purification of recombinant beta-glucanases, in: N.S. Pradeep, L.K. Edison (Eds.), Microbial Beta Glucanases: Molecular Structure, Functions and Applications, Springer Nature, Singapore, Singapore, 2022, pp. 171–185, https://doi.org/10.1007/978-981-19-6466-4_11.

[15] D. Morales, Food by-products and agro-industrial wastes as a source of β-glucans for the formulation of novel nutraceuticals, Pharmaceuticals 16 (2023), https://doi.org/10.3390/ph16030460.

[16] C. Falter, C. Zwikowics, D. Eggert, A. Blümke, M. Naumann, K. Wolff, D. Ellinger, R. Reimer, C.A. Voigt, Glucanocellulosic ethanol: the undiscovered biofuel potential in energy crops and marine biomass, Sci. Rep. 5 (2015), https://doi.org/10.1038/srep13722.

[17] P.F. Ávila, M.F. Silva, M. Martins, R. Goldbeck, Cello-oligosaccharides production from lignocellulosic biomass and their emerging prebiotic applications, World J. Microbiol. Biotechnol. 37 (2021), https://doi.org/10.1007/s11274-021-03041-2.

[18] J.C.G. Cortés, M.Á. Curto, V.S.D. Carvalho, P. Pérez, J.C. Ribas, The fungal cell wall as a target for the development of new antifungal therapies, Biotechnol. Adv. 37 (2019), https://doi.org/10.1016/j.biotechadv.2019.02.008.

[19] Y. Jha, Applications of microbial beta-glucanase in crop improvement under biotic and abiotic stress, in: N.S. Pradeep, L.K. Edison (Eds.), Microbial Beta Glucanases: Molecular Structure, Functions and Applications, Springer Nature, Singapore, Singapore, 2022, pp. 99–116, https://doi.org/10.1007/978-981-19-6466-4_7.

[20] X. Gu, Z. Cao, Z. Li, H. Yu, W. Liu, Plant immunity suppression by an β-1,3-glucanase of the maize anthracnose pathogen Colletotrichum graminicola, BMC Plant Biol. 24 (2024), https://doi.org/10.1186/s12870-024-05053-0.

[21] T. Takashima, N. Komori, K. Uechi, T. Taira, Characterization of an antifungal β-1,3-glucanase from Ficus microcarpa latex and comparison of plant and bacterial β-1,3-glucanases for fungal cell wall β-glucan degradation, Planta 258 (2023), https://doi.org/10.1007/s00425-023-04271-4.

[22] Q. Zeng, J. Xie, Y. Li, X. Chen, X. Gu, P. Yang, G. Hu, Q. Wang, Organization, evolution and function of fengycin biosynthesis gene clusters in the Bacillus amyloliquefaciens group, Phytopathol. Res. 3 (2021), https://doi.org/10.1186/s42483-021-00103-z.

[23] P. Xu, S. Xie, W. Liu, P. Jin, D. Wei, D.G. Yaseen, Y. Wang, W. Miao, Comparative genomics analysis provides new strategies for bacteriostatic ability of Bacillus velezensis HAB-2, Front. Microbiol. 11 (2020), https://doi.org/10.3389/fmicb.2020.594079.

[24] Y. Xue, Y. Zhang, K. Huang, X. Wang, M. Xing, Q. Xu, Y. Guo, A novel biocontrol agent Bacillus velezensis K01 for management of gray mold caused by Botrytis cinerea, AMB Express 13 (2023), https://doi.org/10.1186/s13568-023-01596-x.

[25] V. Choub, H.B. Ajuna, S.J. Won, J.H. Moon, S.I. Choi, C.E.H. Maung, C.W. Kim, Y. S. Ahn, Antifungal activity of Bacillus velezensis ce 100 against anthracnose disease (Colletotrichum gloeosporioides) and growth promotion of walnut (juglans regia L.) trees, Int. J. Mol. Sci. 22 (2021), https://doi.org/10.3390/ijms221910438.

[26] D. Vela-Corcía, D. Aditya Srivastava, A. Dafa-Berger, N. Rotem, O. Barda, M. Levy, MFS transporter from Botrytis cinerea provides tolerance to glucosinolate-breakdown products and is required for pathogenicity, Nat. Commun. 10 (2019) 2886, https://doi.org/10.1038/s41467-019-10860-3.

[27] D. Vela-Corcía, R. Bautista, A. De Vicente, P.D. Spanu, A. Pérez-García, De novo analysis of the epiphytic transcriptome of the cucurbit powdery mildew fungus Podosphaera xanthii and identification of candidate secreted effector proteins, PLoS One 11 (2016) 1–21, https://doi.org/10.1371/journal.pone.0163379.

[28] L.G. Baker, C.A. Specht, M.J. Donlin, J.K. Lodge, Chitosan, the deacetylated form of chitin, is necessary for cell wall integrity in Cryptococcus neoformans, Eukaryot. Cell 6 (2007) 855–867, https://doi.org/10.1128/EC.00399-06.

[29] H. Volk, K. Marton, M. Flajšman, S. Radišek, H. Tian, I. Hein, Č. Podlipnik, B.P.H. J. Thomma, K. Košmelj, B. Javornik, S. Berne, Chitin-binding protein of Verticillium nonalfalfae disguises fungus from plant Chitinases and suppresses chitin-triggered host immunity, Mol. Plant-Microbe Interact. 32 (2019) 1378–1390, https://doi.org/10.1094/MPMI-03-19-0079-R.

[30] J. Jumper, R. Evans, A. Pritzel, T. Green, M. Figurnov, O. Ronneberger, K. Tunyasuvunakool, R. Bates, A. Žídek, A. Potapenko, A. Bridgland, C. Meyer, S.A. A. Kohl, A.J. Ballard, A. Cowie, B. Romera-Paredes, S. Nikolov, R. Jain, J. Adler, T. Back, S. Petersen, D. Reiman, E. Clancy, M. Zielinski, M. Steinegger, M. Pacholska, T. Berghammer, S. Bodenstein, D. Silver, O. Vinyals, A.W. Senior, K. Kavukcuoglu, P. Kohli, D. Hassabis, Highly accurate protein structure prediction with AlphaFold, Nature 596 (2021) 583–589, https://doi.org/10.1038/s41586-021-03819-2.

[31] A. Grosdidier, V. Zoete, O. Michielin, SwissDock, a protein-small molecule docking web service based on EADock DSS, Nucleic Acids Res. 39 (2011) W270–W277, https://doi.org/10.1093/nar/gkr366.

[32] A. Grosdidier, EADock: docking of small molecules into protein active sites with a multiobjective evolutionary optimization, Proteins Struct. 1025 (2007) 1010–1025, https://doi.org/10.1002/prot.

[33] M.J. Bailey, P. Biely, K. Poutanen, Interlaboratory Testing of Methods for Assay of Xylanase Activity, 1992.

[34] R. Wang, Z. Long, X. Liang, S. Guo, N. Ning, L. Yang, X. Wang, B. Lu, J. Gao, The role of a β-1,3-1,4-glucanase derived from Bacillus amyloliquefaciens FS6 in the protection of ginseng against Botrytis cinerea and Alternaria panax, Biol. Control 164 (2021), https://doi.org/10.1016/j.biocontrol.2021.104765.

[35] S.-I. Choi, H.-I. Lim, H.B. Ajuna, J.-H. Moon, S.-J. Won, V. Choub, J.-Y. Yun, Y. Sang Ahn, Biocontrol of fungal pathogens and growth promotion in the Korean fir (Abies koreana E.H.Wilson) seedling using *Bacillus velezensis* CE 100, Biol. Control (2024) 105620, https://doi.org/10.1016/j.biocontrol.2024.105620.

[36] M. Zhao, D. Liu, Z. Liang, K. Huang, X. Wu, Antagonistic activity of Bacillus subtilis CW14 and its β-glucanase against Aspergillus ochraceus, Food Control 131 (2022), https://doi.org/10.1016/j.foodcont.2021.108475.

[37] G. Steinberg, M.A. Peñalva, M. Riquelme, H.A. Wösten, S.D. Harris, Cell biology of hyphal growth, Microbiol. Spectr. 5 (2017), https://doi.org/10.1128/microbiolspec.funk-0034-2016.

[38] K. Miyazawa, A. Yoshimi, A. Yoshimi, K. Abe, K. Abe, K. Abe, The mechanisms of hyphal pellet formation mediated by polysaccharides, α-1,3-glucan and galactosaminogalactan, in Aspergillus species, Fungal Biol. Biotechnol. 7 (2020), https://doi.org/10.1186/s40694-020-00101-4.

[39] K.F. Mitchell, R. Zarnowski, D.R. Andes, The extracellular matrix of fungal biofilms, Adv. Exp. Med. Biol. 931 (2016) 21–35, https://doi.org/10.1007/5584_2016_6.

[40] M. Lorito, C. Peterbauer, C.K. Hayes, G.E. Harman, Synergistic interaction between fungal cell wall degrading enzymes and different antifungal compounds enhances inhibition of spore germination, 1994.

[41] A.O. Chizhov, Y.E. Tsvetkov, N.E. Nifantiev, Gas-phase fragmentation of cyclic oligosaccharides in tandem mass spectrometry, Molecules 24 (2019), https://doi.org/10.3390/molecules24122226.

[42] D. Veličković, D. Ropartz, F. Guillon, L. Saulnier, H. Rogniaux, New insights into the structural and spatial variability of cell-wall polysaccharides during wheat grain development, as revealed through MALDI mass spectrometry imaging, J. Exp. Bot. 65 (2014) 2079–2091, https://doi.org/10.1093/jxb/eru065.

[43] S.G. Grishutin, A.V. Gusakov, E.I. Dzedzyulya, A.P. Sinitsyn, A lichenase-like family 12 endo-(1→4)-β-glucanase from Aspergillus japonicus: study of the substrate specificity and mode of action on β-glucans in comparison with other glycoside hydrolases, Carbohydr. Res. 341 (2006) 218–229, https://doi.org/10.1016/j.carres.2005.11.011.

[44] T.T. Xie, J. Shen, Z. Geng, F. Wu, Y. Dong, Z. Cui, Y. Liang, X. Ye, Antifungal characterizations of a novel endo-β-1,6-glucanase from Flavobacterium sp. NAU1659, Appl. Microbiol. Biotechnol. 108 (2024), https://doi.org/10.1007/s00253-024-13269-1.

[45] T. Zhou, S. Yu, H. Xu, H. Liu, Y. Rao, Stimulating fungal cell wall integrity by exogenous β-glucanase to improve the production of fungal natural products, Appl. Microbiol. Biotechnol. 106 (2022) 7491–7503, https://doi.org/10.1007/s00253-022-12224-2.

[46] C. Chaliha, M.D. Rugen, R.A. Field, E. Kalita, Glycans as modulators of plant defense against filamentous pathogens, Front. Plant Sci. 9 (2018), https://doi.org/10.3389/fpls.2018.00928.

[47] N. Amarsaikhan, S.P. Templeton, Co-recognition of β-glucan and chitin and programming of adaptive immunity to Aspergillus fumigatus, Front. Microbiol. 6 (2015), https://doi.org/10.3389/fmicb.2015.00344.

[48] P. Nisha, Beta-glucanase: diverse bacterial sources and its applications, in: N. S. Pradeep, L.K. Edison (Eds.), Microbial Beta Glucanases: Molecular Structure, Functions and Applications, Springer Nature, Singapore, Singapore, 2022, pp. 33–49, https://doi.org/10.1007/978-981-19-6466-4_3.

[49] X. Jin, J.K. Wang, Q. Wang, Microbial β-glucanases: production, properties, and engineering, World J. Microbiol. Biotechnol. 39 (2023), https://doi.org/10.1007/s11274-023-03550-2.

[50] Z. Huang, G. Ni, X. Zhao, F. Wang, M. Qu, Characterization of a GH8 β-1,4-glucanase from Bacillus subtilis B111 and its Saccharification potential for agricultural straws, J. Microbiol. Biotechnol. 31 (2021) 1446–1454, https://doi.org/10.4014/jmb.2105.05026.
[51] S. Kaur, M.K. Samota, M. Choudhary, M. Choudhary, A.K. Pandey, A. Sharma, J. Thakur, How do plants defend themselves against pathogens-biochemical mechanisms and genetic interventions, Physiol. Mol. Biol. Plants 28 (2022) 485–504, https://doi.org/10.1007/s12298-022-01146-y.
[52] C. dos Santos, O.L. Franco, Pathogenesis-related proteins (PRs) with enzyme activity activating plant defense responses, Plants 12 (2023), https://doi.org/10.3390/plants12112226.
[53] A.K. Wani, N. Akhtar, F. Sher, A.A. Navarrete, J.H.P. Américo-Pinheiro, Microbial adaptation to different environmental conditions: molecular perspective of evolved genetic and cellular systems, Arch. Microbiol. 204 (2022), https://doi.org/10.1007/s00203-022-02757-5.
[54] J. Wang, J.A. Stuckey, M.J. Wishart, J.E. Dixon, A unique carbohydrate binding domain targets the Lafora disease phosphatase to glycogen, J. Biol. Chem. 277 (2002) 2377–2380, https://doi.org/10.1074/jbc.C100686200.
[55] C. Caseiro, J.N.R. Dias, C.M.G. de Andrade Fontes, P. Bule, From Cancer therapy to winemaking: the molecular structure and applications of β-glucans and β-1, 3-glucanases, Int. J. Mol. Sci. 23 (2022), https://doi.org/10.3390/ijms23063156.
[56] R.M. Yennamalli, A.J. Rader, J.D. Wolt, T.Z. Sen, Thermostability in endoglucanases is fold-specific, BMC Struct. Biol. 11 (2011), https://doi.org/10.1186/1472-6807-11-10.
[57] A.I. Witek, K. Witek, J. Hennig, Conserved Cys Residue Influences Catalytic Properties of Potato Endo-(1-3)-β-glucanase GLUB20-2. www.actabp.pl, 2008.
[58] J. Ma, Z. Jiang, Q. Yan, A. Lv, Y. Li, S. Yang, Structural and functional analysis of SpGlu64A: a novel glycoside hydrolase family 64 laminaripentaose-producing β-1,3-glucanase from Streptomyces pratensis, FEBS J. 291 (2024) 2009–2022, https://doi.org/10.1111/febs.17094.
[59] J.M. Raaijmakers, I. de Bruijn, O. Nybroe, M. Ongena, Natural functions of lipopeptides from Bacillus and Pseudomonas: more than surfactants and antibiotics, FEMS Microbiol. Rev. 34 (2010) 1037–1062, https://doi.org/10.1111/j.1574-6976.2010.00221.x.
[60] M.R. Kao, J. Parker, D. Oehme, S.C. Chang, L.C. Cheng, D. Wang, V. Srivastava, J. M. Wagner, P.J. Harris, Y.S.Y. Hsieh, Substrate specificities of variants of barley (1,3)- and (1,3;1,4)-β-d-Glucanases resulting from mutagenesis and segment hybridization, Biochemistry 63 (2024) 1194–1205, https://doi.org/10.1021/acs.biochem.3c00673.
[61] J.J. Chen, X. Liang, T.J. Chen, J.L. Yang, P. Zhu, Site-directed mutagenesis of a β-glycoside hydrolase from *Lentinula edodes*, Molecules 24 (2019), https://doi.org/10.3390/molecules24010059.
[62] V.N. Monteiro, C.J. Ulhoa, Biochemical characterization of a β-1,3-glucanase from Trichoderma koningii induced by cell wall of Rhizoctonia solani, Curr. Microbiol. 52 (2006) 92–96, https://doi.org/10.1007/s00284-005-0090-2.
[63] K.R.S. Celestino, R.B. Cunha, C.R. Felix, Characterization of a β-glucanase produced by Rhizopus microsporus var. microsporus, and its potential for application in the brewing industry, BMC Biochem. 7 (2006), https://doi.org/10.1186/1471-2091-7-23.
[64] E.F. Noronha, C.J. Ulhoa, Characterization of a 29-kDa Ì2-1,3-glucanase from Trichoderma harzianum, FEMS Microbiol. Lett. 183 (2000) 119–123, https://doi.org/10.1111/j.1574-6968.2000.tb08944.x.
[65] Y. Jiang, H. Xu, Y. Li, H. Liu, L. Yu, M. Qiao, G. Liu, Draft genome sequence of Bacillus subtilis strain NKYL29, an antimicrobial-peptide-producing strain from soil, Genome Announc. 2 (2014), https://doi.org/10.1128/genomeA.01140-14.
[66] M.C. Magno-Perez-Bryan, P.M. Martinez-Garcia, J. Hierrezuelo, P. Rodriguez-Palenzuela, E. Arrebola, C. Ramos, A. De Vicente, A. Perez-Garcia, D. Romero, Comparative genomics within the bacillus genus reveal the singularities of two robust bacillus amyloliquefaciens biocontrol strains, Mol. Plant-Microbe Interact. 28 (2015) 1102–1116, https://doi.org/10.1094/MPMI-02-15-0023-R.
[67] Z. Huang, G. Ni, F. Wang, X. Zhao, Y. Chen, L. Zhang, M. Qu, Characterization of a thermostable Lichenase from Bacillus subtilis B110 and its effects on β-glucan hydrolysis, J. Microbiol. Biotechnol. 32 (2022) 484–492, https://doi.org/10.4014/jmb.2111.11017.
[68] J. Wang, Y. Wang, X. Wang, D. Zhang, S. Wu, G. Zhang, Enhanced thermal stability of lichenase from Bacillus subtilis 168 by SpyTag/SpyCatcher-mediated spontaneous cyclization, Biotechnol. Biofuels 9 (2016), https://doi.org/10.1186/s13068-016-0490-5.
[69] J.M. Eklöf, H. Brumer, The XTH gene family: an update on enzyme structure, function, and phylogeny in xyloglucan remodeling, Plant Physiol. 153 (2010) 456–466, https://doi.org/10.1104/pp.110.156844.
[70] A.H. Viborg, N. Terrapon, V. Lombard, G. Michel, M. Czjzek, B. Henrissat, H. Brumer, A subfamily roadmap of the evolutionarily diverse glycoside hydrolase family 16 (GH16), J. Biol. Chem. 294 (2019) 15973–15986, https://doi.org/10.1074/jbc.RA119.010619.
[71] G.P. Furtado, S. Carli, L.P. Meleiro, J.C.S. Salgado, R.J. Ward, Enhanced hydrolytic efficiency of an engineered CBM11-glucanase enzyme chimera against barley β-D-glucan extracts, Food Chem. 365 (2021), https://doi.org/10.1016/j.foodchem.2021.130460.
[72] A.H. Teh, N.H. Fazli, G. Furusawa, Crystal structure of a neoagarobiose-producing GH16 family β-agarase from Persicobacter sp. CCB-QB2, Appl. Microbiol. Biotechnol. 104 (2020) 633–641, https://doi.org/10.1007/s00253-019-10237-y.
[73] M. Hahn, J. Pons, A. Planas, E. Querol, U. Heinemann, Crystal structure of Bacillus licheniformis 1,3-1,4-β-d-glucan 4-glucanohydrolase at 1.8 Å resolution, FEBS Lett. 374 (1995) 221–224, https://doi.org/10.1016/0014-5793(95)01111-Q.
[74] Q. Deng, R. Wang, D. Sun, L. Sun, Y. Wang, Y. Pu, Z. Fang, D. Xu, Y. Liu, R. Ye, S. Yin, S. Xie, R. Gooneratne, Complete genome of Bacillus velezensis CMT-6 and comparative genome analysis reveals Lipopeptide diversity, Biochem. Genet. 58 (2020) 1–15, https://doi.org/10.1007/s10528-019-09927-z.
[75] H. Westers, R. Dorenbos, J.M. Van Dijl, J. Kabel, T. Flanagan, K.M. Devine, F. Jude, S.J. Séror, A.C. Beekman, E. Darmon, C. Eschevins, A. De Jong, S. Bron, O. P. Kuipers, A.M. Albertini, H. Antelmann, M. Hecker, N. Zamboni, U. Sauer, C. Bruand, D.S. Ehrlich, J.C. Alonso, M. Salas, W.J. Quax, Genome engineering reveals large dispensable regions in Bacillus subtilis, Mol. Biol. Evol. 20 (2003) 2076–2090, https://doi.org/10.1093/molbev/msg219.